JAERI-Tech
2002-032

PERFORMANCE TEST OF MICRO-FISSION CHAMBERS FOR IN-VESSEL NEUTRON MONITORING OF ITER

March 2002

Michinori YAMAUCHI, Takeo NISHITANI, Kentaro OCHIAI,
Yuichi MORIMOTO, Jun-ichi HORI, Katsuyuki EBISAWA
and Satoshi KASAI

日本原子力研究所
Japan Atomic Energy Research Institute

本レポートは，日本原子力研究所が不定期に公刊している研究報告書です。
入手の問合わせは，日本原子力研究所研究情報部研究情報課（〒319－1195 茨城県那珂郡東海村）あて，お申し越しください。なお，このほかに財団法人原子力弘済会資料センター（〒319－1195 茨城県那珂郡東海村日本原子力研究所内）で複写による実費頒布をおこなっております。

This report is issued irregularly.
Inquiries about availability of the reports should be addressed to Research Information Division, Department of Intellectual Resources, Japan Atomic Energy Research Institute, Tokai-mura, Naka-gun, Ibaraki-ken 〒319－1195, Japan.

編集兼発行　日本原子力研究所

JAERI-Tech 2002-032

Performance Test of Micro-fission Chambers for In-vessel Neutron Monitoring of ITER

Michinori YAMAUCHI, Takeo NISHITANI, Kentaro OCHIAI, Yuichi MORIMOTO, Jun-ichi HORI, Katsuyuki EBISAWA+ and Satoshi KASAI

Department of Fusion Engineering Research
(Tokai Site)
Naka Fusion Research Establishment
Japan Atomic Energy Research Institute
Tokai-mura, Naka-gun, Ibaraki-ken

(Received January 30, 2002)

A micro-fission chamber with 12 mg UO_2 and a dummy chamber without uranium were fabricated and the performance was tested. They are designed to be installed inside the vacuum vessel of the compact ITER (ITER-FEAT) for neutron monitoring. The vacuum leak rate of the dummy chamber with MI cable, resistances of chambers between central conductor and outer sheath, and mechanical strength up to 50G acceleration were confirmed to meet the design criteria. The gamma-ray sensitivity was measured for the dummy chamber with the ^{60}Co gamma-ray irradiation facility at JAERI Takasaki. The output signals for gamma-rays in Campbelling mode were estimated to be less than 0.1 % of those by neutrons at the location behind the blanket module in ITER-FEAT. The detector response for 14 MeV neutrons was investigated with the FNS facility. Excellent linearity between count rates, square of Campbelling voltage and neutron fluxes was confirmed in the temperature range from 20°C(room) to 250°C. However, a positive dependence of 14 MeV neutron count rates on temperature was observed, which might be caused by the increase in the pulse height with temperature rise. Effects of a change of surrounding materials were evaluated by the sensitivity measurements of the micro-fission chamber inserted into the shielding blanket mock-up. The sensitivity was enhanced by slow-downed neutrons, which agreed with the calculation result by MCNP-4C code. As a result, it was concluded that the developed micro-fission chamber is applicable for ITER-FEAT.

Keywords: Neutron Monitor, Micro-fission Chamber, ITER, Fusion Power, Neutron Source Intensity, Campbelling Mode, ^{60}Co Gamma-ray Irradiation Facility, Fusion Neutronics Source(FNS)

This work is conducted as an ITER Engineering Activities as this report corresponds to ITER R&D Task Agreement on "Microfission chamber flux monitor" (N 55 TT 07 FJ).

+ Department of ITER Project (Present address: Toshiba Corporation)

ITER 真空容器内中性子モニターのためのマイクロフィッションチェンバーの性能試験

日本原子力研究所那珂研究所核融合工学部
山内 通則・西谷 健夫・落合 謙太郎・森本 裕一
堀 順一・海老澤 克之+・河西 敏

(2002 年 1 月 30 日受理)

ITER(ITER-FEAT)真空容器内の中性子モニターの開発を目的として、12mg の二酸化ウランを用いたマイクロフィッションチェンバーとウランのないダミーチェンバーを製作し、性能試験を行った。基本性能として、MI ケーブルを取り付けたダミーチェンバーの真空リーク率、チェンバー内の導体と外側容器の絶縁性能、50G までの加速度に対する耐性はいずれも設計要求条件を満たした。ガンマ線に対する感度試験は日本原子力研究所高崎研究所の ^{60}Co ガンマ線照射装置によって行った。それによれば、ITER-FEAT ブランケット背後の環境で、ガンマ線に対する感度は中性子に対する感度の 0.1%以下と評価できた。また 14MeV 中性子に対する検出器の応答は東海研究所の核融合中性子源(FNS)によって試験した。その結果、20°C(室温)から 250°C までの範囲で計数率及びキャンベル出力の二乗と中性子束の良好な直線性が確認できた。ただし、14MeV 中性子の計数率が温度の上昇と共に増加する現象が観測され、パルスの高さが温度と共に大きくなる傾向があることがわかった。遮蔽体がある場合の検出器応答は遮蔽ブランケットの模擬体を用いて試験を行い、MCNP 計算の結果と良く一致したデータが得られた。それによると中性子の減速により検出器の感度は上昇するが、遮蔽体の変動による感度の変化は小さい。結論として、本マイクロフィッションチェンバーは ITER-FEAT の中性子モニターとして充分な性能を有することがわかった。

本研究はＩＴＥＲ工学設計活動の一環として実施したもので、本報告はＲ＆Ｄタスク協定(N 55 TT 07 FJ)に基づくものである。

那珂研究所(東海駐在):〒319-1195 茨城県那珂郡東海村白方白根 2-4
+ ITER 開発室(現(株)東芝)

Contents

目　次

1. INTRODUCTION

1.1 Background and objectives

The measurement of absolute neutron source intensity is very important for controlling the fusion power of ITER. In present large Tokamaks, neutron flux monitors are installed inside and outside the vacuum vessel for this purpose, but the detection efficiencies of these detectors are easily affected by surrounding materials. Since ITER has substantial material outside the plasma core, a close position is preferred for the neutron flux monitors.

A micro fission chamber is a pencil size gas counter with fissile material inside, which was developed as an in-core monitor for fission reactors. However, the surrounding environment is quite different from nuclear power plants where these fission chambers have been implemented, and R & D is required to establish their applicability to ITER.

In the ITER CDA (Conceptual Design Activity), we planned to install micro-fission chambers just under the first wall [1]. However, that is rather difficult because nuclear heating will be more than 10 W/cm^3, and burn-up of the fissile material will reduce the life time of the detector. In the ITER-FDR, the detectors will be installed in the gap between adjacent blanket modules and behind the blanket on the back plate [2-4]. For ITER-FEAT, a ^{235}U micro-fission chamber and a "blank" detector which is a fissile-material-free detector to identify noise issues such as from gamma-rays will be installed behind blankets #11 and #16 in a toroidal location [5]. We propose two toroidal locations from the redundancy point of view. Employing both pulse counting mode and Campbelling mode in the electronics, we can accomplish the ITER requirement that the temporal resolution is to be 1 ms for the dynamic range of 10^4. According to the lifetime estimation of the micro fission chamber, the change of the sensitivity will be only 0.1 % for the ITER lifetime which is equivalent to 0.5 GW•year. So, we can use the ^{235}U chambers without replacement during ITER lifetime. The micro fission chamber system can meet the required 10% accuracy for a fusion power monitor.

The objectives of this R&D are to fabricate a prototype micro fission chamber and to test it under ITER relevant conditions including wide neutron spectrum, intense high gamma rays, and acceleration to simulate sudden disruption. The data will be evaluated to support the engineering design of ITER.

1.2 Technical Outline of the Task

This task requires the fabrication of one micro fission chamber and one chamber without fission materials at a designated specification. Following R&D tests items should be carried out at the neutron source facilities and/or intense gamma-ray source facilities in JAERI. And the documentation of the test results and evaluations are as follows.

R&D test items;

1) Characterizing the measurement capability under neutron and/or gamma-ray irradiation.
2) Characterizing the measurement capability under various temperature conditions, accelerations.
3) Comparison of signal levels with the chamber having no fission material.
4) Examining the effect of surrounding materials

Performance Tests;

1) Dimensional check, vacuum test including MI cables.
2) Static impedance test and temperature dependence test up to 350 °C.
3) Acceleration test by mechanical shocks.
4) Neutron flux measurement using FNS [6] from the available maximum flux to the possible minimum flux including linearity and S/N dependence on the wide dynamic range.
5) Neutron flux measurement using FNS at elevated temperature.
6) Effects of the change of surrounding materials in Test 5.
7) Gamma-ray irradiation test using ^{60}Co source on the chamber having no fissionable material and noise level dependence on elevated temperatures.

2. SPECIFICATION OF THE MICRO FISSION CHAMBERS

The micro fission chamber should be operated in pulse counting mode at low neutron flux, in Campbelling (mean square voltage) mode [7] at medium flux, and in current mode at high flux. Combinations of those operation modes may provide a dynamic range of 10^{10} with a temporal resolution of 1 ms. The most popular candidates for the fissile material in a micro fission chamber are ^{235}U and ^{238}U. The former has a large fission cross-section for thermal neutrons, while the latter has a fission cross section with a threshold of ~0.8 MeV.

Mineral insulated (MI) cable is used to transfer signals, so that we can install the micro-fission chambers inside the vacuum vessel in the same manner as magnetic probes. Cooling of the detectors is necessary in order to keep the operational temperature below 300°C in the presence of strong nuclear heating inside the vacuum vessel.

In order to get a wide dynamic range, the fission reaction rate during maximum power operation of ITER should be as high as the operational limit of the detector. The maximum fission reaction rate of this type of chamber is 10^{10} s^{-1} for the Campbelling mode.

Specifications of the micro fission chambers are listed as follows;

1) Length:	200 mm
2) Diameter:	14 mm
3) Fissionable material:	a) $^{235}U O_2$ 10mg or below the over coating level
	b) dummy, no fissionable material
4) Temperature:	20 -200 °C
	200 - 350 °C /hr for 10 times
5) Acceleration:	15 G, 10 ms for 1000 times or equivalent
6) Accuracy for total neutron yield:	10 %
7) Time resolution:	1 ms
8) Dynamic range:	10^7
9) Gamma-rays back ground:	10 times of neutron flux
10) Pressure:	High vacuum

3. FABRICATION OF MICRO FISSION CHAMBER AND DUMMY CHAMBER

3.1 Design of the Micro Fission Chamber and the Dummy Chamber

Figure 3.1-1 shows the schematics of a typical micro fission chamber with wide dynamic range, which is designed for the ITER-FEAT. In this detector, UO_2 is coated on the outer cylindrical electrode with a coating density of 0.6 mg/cm^2. The active length is 76 mm, and the total amount of UO_2 is 12 mg. The enrichment of ^{235}U is 90%. So the total amount of ^{235}U is about 10 mg. This detector is filled with 14.6 atm. of Ar + 5% N_2 gas, which enables pulse counting and Campbelling mode. The housing material is stainless steel 316L. Electric insulator is alumina (Al_2O_3).

Double coaxial MI cable is welded directly to the fission chamber. The MI cable uses SiO_2 as electric insulator with a packing density of 30%. The cable is also filled with Ar at 14.6 atm. The center conductor is insulated not only with the SiO_2 power but also Ar gas. In case of cracking at the alumina insulator in the detector due to swelling, the Ar gas in the MI cable will prevent a leak of detector gas into the MI cable.

The dummy chamber has the same structure as the micro fission chamber, except no uranium coating on the electrode.

3.2 Fabrication

A drawing of the fabricated micro fission chamber is shown in Figure 3.2-1. Dimensions at "A" - "D" are checked at the dimension test described in Section 4.1. Also a photograph is shown in Figure 3.2-2. The total length of the fission chamber is 5 m including MI cable. The end of the MI cable has a connector, which is LEMO type quick coupling connector for a soft double coaxial cable.

The chamber was baked and pumped out to vacuum from the gas feeder tube at the detector head. After that gas of Ar + 5% N_2 was filled up to 14.6 atm and the gas feeder tube was welded.

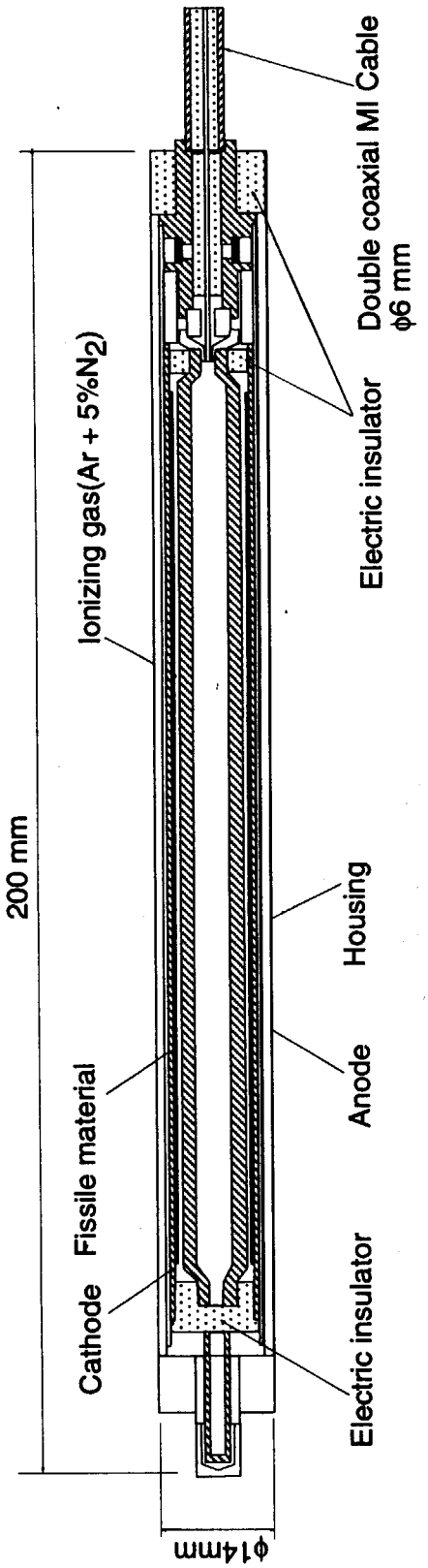

Figure 3.1-1 Schematics of Micro fission chamber

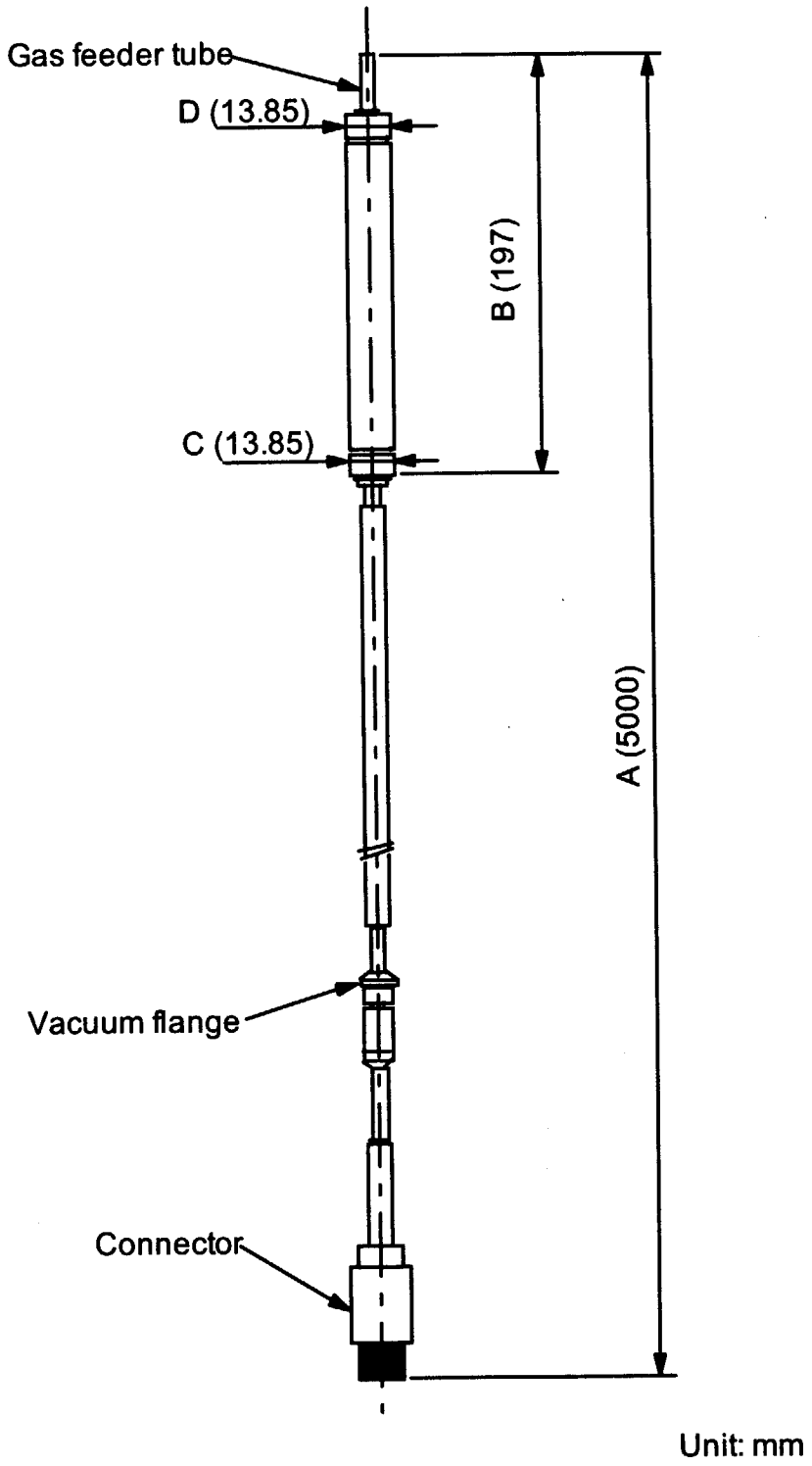

Figure 3.2-1 Drawing of the fabricated micro fission chamber and the dummy chamber.

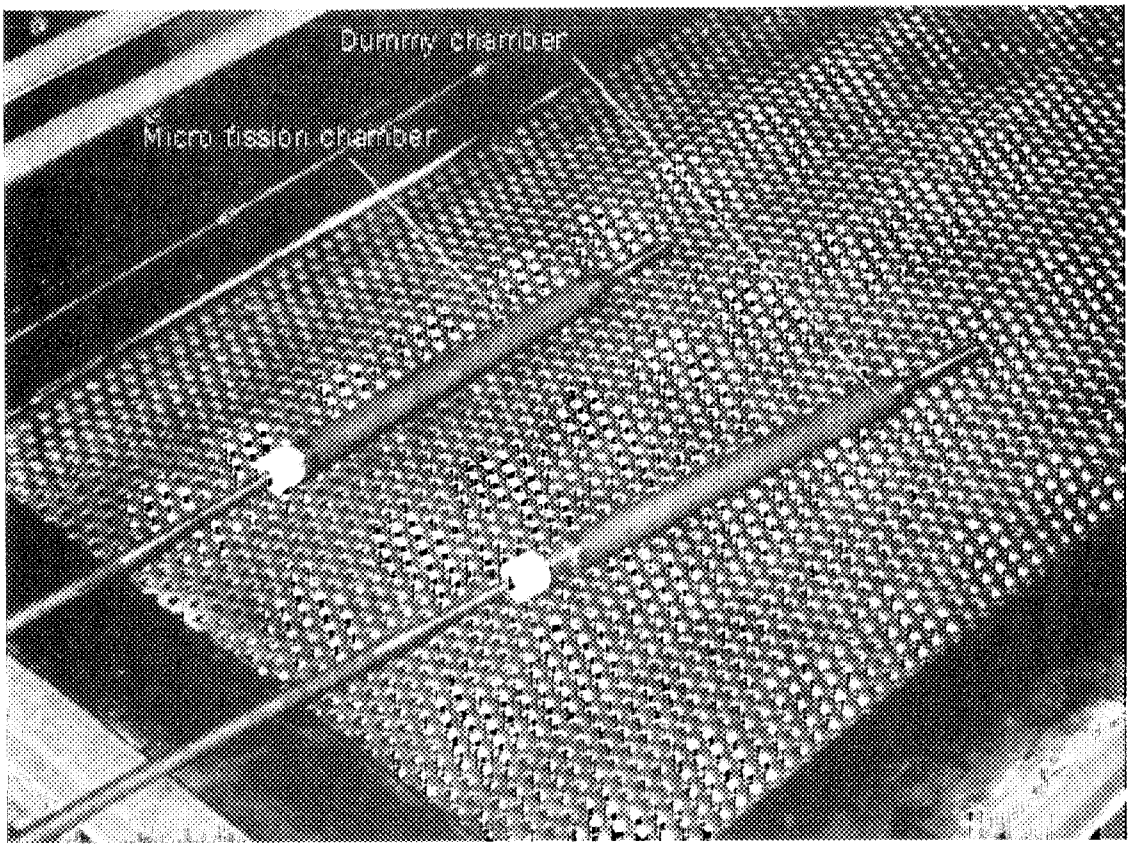

Figure 3.2-2 Picture of the fabricated micro fission chamber and the dummy chamber.

4. BASIC PERFORMANCE TESTS

4.1 Dimension Check

The result of the dimension check is shown in Table 4.1-1. The measured dimension agreed with the designed one within the permitted error. The position B has a relatively large permitted error, because the gas feeder tube was welded after filling the Ar + 5% N_2 gas into the detector.

4.2 Vacuum Leak Test

The dummy chamber with MI cable was tested for vacuum leaks at room temperature. We confirmed that the He leak rate was less than the detection limit, 1×10^{-8} cc/s.

4.3 Static Impedance Test

The resistance between the center conductor and the outer sheath was measured in the temperature range from room temperature (20°C) to 350°C with an impedance analyser. The detector heads of the micro fission chamber and the dummy chamber were heated up by a heater chamber as shown in Figure 4.3-1. The temperature history is shown in Figure 4.3-2. The temperature dependence of the resistance is shown in Table 4.3-1 and Figure 4.3-3. The measured resistance of the micro fission chamber is larger than that of the dummy chamber at low temperatures, because the conductivity is increased by the alpha particle ionization from the alpha decay of the uranium. In the higher temperature range, the resistance is determined by the increased conductance of the ceramic insulator itself. Those measured resistances are within the acceptable range for the micro fission chamber performance.

4.4 Pulse Height Discrimination Characteristics

The pulse height discrimination characteristics of the micro fission chamber was investigated in the temperature range from room temperature (20°C) to 350°C. The block diagram of the electronics is shown in Figure 4.4-1. In this measurement, only the pulse output was used. The temperature history was the same as shown in Figure 4.3-2. The pulse height discrimination characteristics for the thermal noise and alpha particle of the uranium

itself are shown in Table 4.4-1 and Figure 4.4-2. Pulses smaller than 60 mV are thermal noise. Those larger than 60 mV are due to alpha particle of the uranium. Also Figure 4.4-3 shows the temperature dependence of the count rate at several discrimination levels. The thermal noise component is insensitive to the temperature. However, the count rate due to alpha particles increases with the temperature, which indicates positive temperature dependence of the pulse height.

During the neutron measurement, the discriminator should eliminate counts due the alpha decay of the uranium. The discrimination level should be higher than -150 mV.

4.5 Acceleration Test

The micro fission chambers will be installed inside the vacuum vessel. Those chambers have to bear the mechanical shock at disruptions. We carried out the acceleration test by mechanical shocks. The micro fission chamber was set on a weighted free-fall table as shown in Figure 4.5-1. A picture of the experimental setup is shown in Figure 4.5-2. When the table hit the floor, the acceleration was 50G. The waveform of the acceleration is shown in Figure 4.5-3. We carried out this acceleration test 10 times. Counts of 34 - 71 were observed during each mechanical shock, where the discrimination level was -200 mV. On the other hand, there was no change in the Campbelling output signal. Also any change in resistance, dimension and vacuum leaks were not observed. Counts of 34 - 71 are negligible small in the real ITER measurement, so we can conclude that the micro fission chamber can be used under the mechanical condition of ITER.

4.6 Discrimination Characteristics and Sensitivity for Thermal Neutrons

The discrimination characteristics and the sensitivity for thermal neutrons were investigated at the TRIG reactor of the Rikkyo University, Yokosuka. The neutron flux was $6.76 \times 10^5\,cm^{-2}\,s^{-1}$ at 20 W reactor power. The discrimination characteristics is shown in Figure 4.6-1. The count rate was almost flat in the range of the discrimination level from -80 mV to -200 mV. We should set the discrimination level to be -150 mV to -200 mV, taking the results of the Section 4.4 into account.

At the discrimination level of -200 mV, the thermal neutron sensitivity was evaluated to be $1.04 \times 10^{-2}\,counts/(cm^{-2}\,s^{-1})$.

Table 4.1-1 Result of the dimension check.

Position	A [mm]	B[mm]	C[mm]	D[mm]
Designed value	5000±20	197±2	13.85±0.1	13.85±0.1
Measured value	4998	197.3	13.85	13.86

See Figure 3.2-1 for the positions A-B.

Table 4.3-1 Resistance between the center conductor and the outer sheath.

Temperature (°C)	R.T.(20)	100	150	250	350	R.T.(20)
Micro fission chamber (Ω)	2.7×10^{12}	9.0×10^{11}	6.0×10^{11}	1.0×10^{11}	1.5×10^{10}	2.5×10^{12}
Dummy chamber (Ω)	1.2×10^{13}	2.0×10^{12}	4.0×10^{11}	1.0×10^{11}	2.4×10^{10}	1.0×10^{13}

Table 4.4-1 The pulse height discrimination characteristics of the micro fission chamber for the thermal noise and alpha particle of the uranium itself.

Temperature (degree C)	R.T. (20)	100	150	200	250	R.T. (20)
Discri[-mV]	Count rate (cps)	Count rate (cps)	Count rate (cps)	Count rate (cps)	Count rate (cps)	Count rate (cps)
0	2.80E+06	2.86E+06	2.87E+06	2.87E+06	2.81E+06	2.78E+06
10	1.09E+06	1.05E+06	1.05E+06	1.02E+06	1.01E+06	1.00E+06
20	3.10E+05	2.71E+05	2.68E+05	2.49E+05	3.20E+05	2.54E+05
30	5.05E+04	4.21E+04	4.38E+04	3.63E+04	5.97E+04	3.86E+04
40	8.39E+03	5.43E+03	5.34E+03	4.29E+03	8.67E+03	4.60E+03
50	9.54E+02	7.74E+02	7.82E+02	7.81E+02	1.20E+03	5.60E+02
60	1.72E+02	2.30E+02	2.18E+02	3.48E+02	3.20E+02	1.53E+02
70	5.00E+01	1.92E+02	9.89E+01	2.24E+02	1.62E+02	4.49E+01
80	2.30E+01	4.20E+01	3.40E+01	1.32E+02	1.05E+02	1.40E+01
90	7.98E+00	2.40E+01	6.00E+00	7.30E+01	4.49E+01	2.00E+00
100	2.00E+00	2.00E+00	1.99E+00	8.00E+00	1.79E+01	1.00E+00
110	0.00E+00	1.00E+00	0.00E+00	2.99E+00	6.99E+00	0.00E+00
120	0.00E+00	0.00E+00	0.00E+00	1.00E+00	2.00E+00	0.00E+00
130	0.00E+00	0.00E+00	0.00E+00	0.00E+00	0.00E+00	0.00E+00

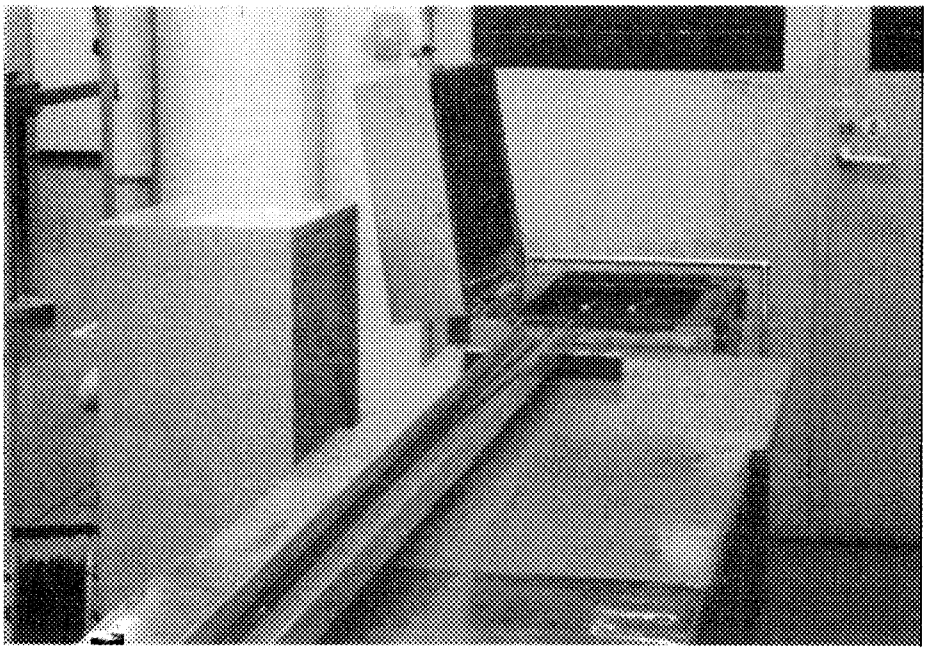

Figure 4.3-1 Picture of the temperature tests for the micro fission chamber and the dummy chamber.

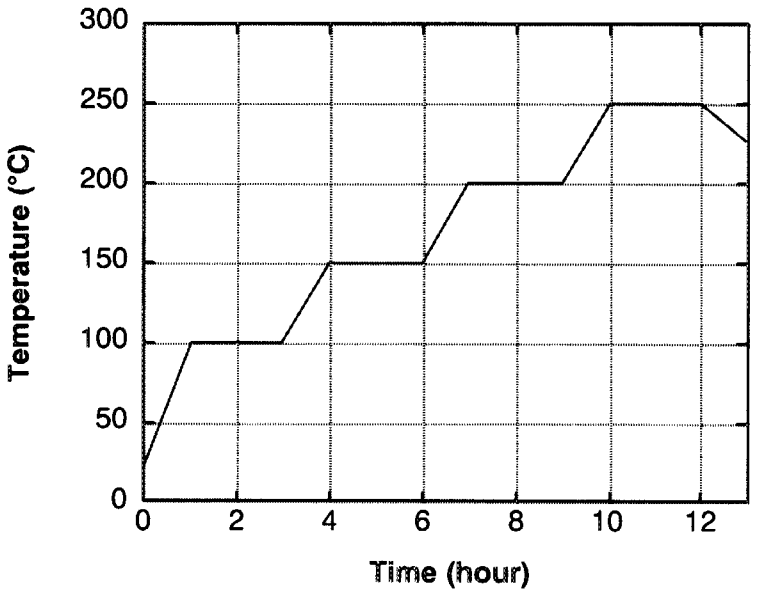

Figure 4.3-2 Temperature history of the temperature tests for the micro fission chamber and the dummy chamber.

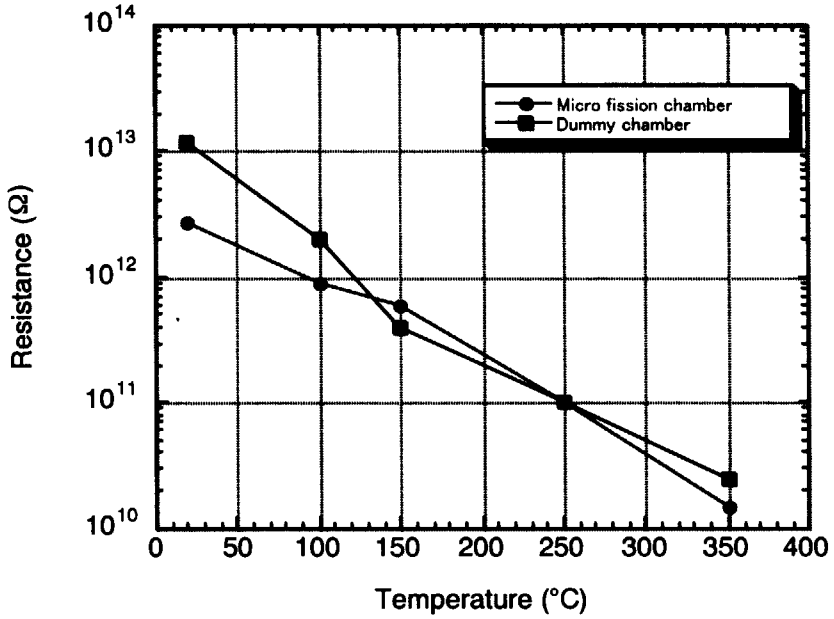

Figure 4.3-3 The temperature dependence of the resistance between the center conductor and the outer sheath.

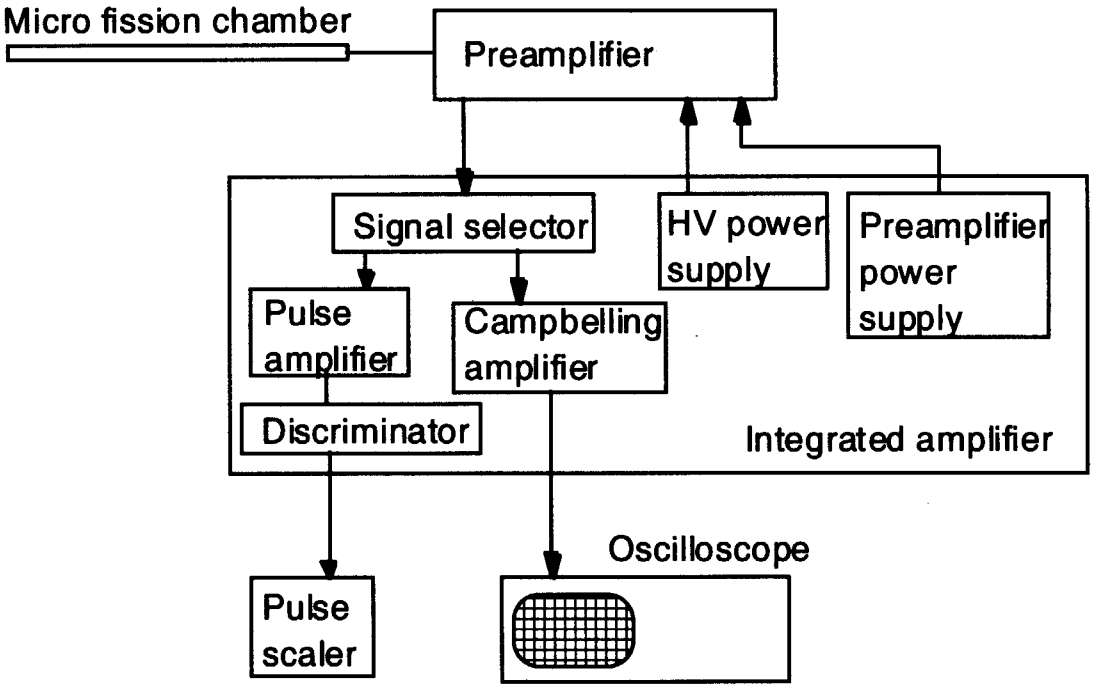

Figure 4.4-1 Block diagram of the electronics for the micro fission chamber.

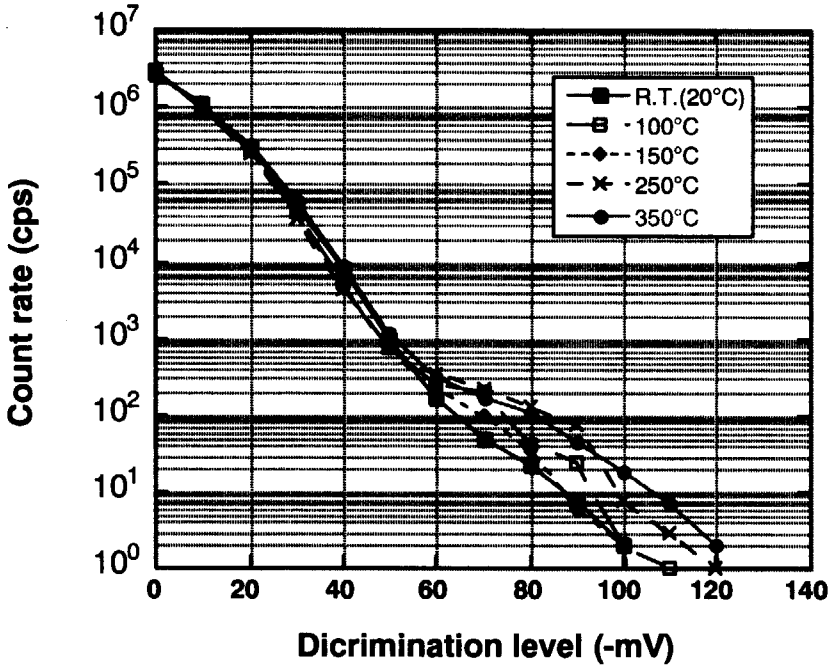

Figure 4.4-2 Pulse height discrimination characteristics of the micro fission chamber for thermal noise and alpha particles of the uranium.

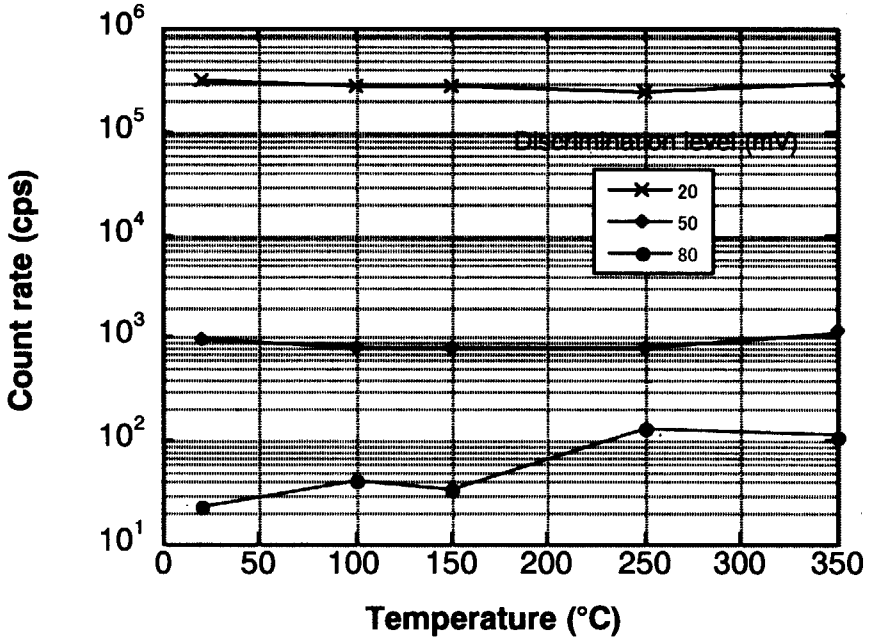

Figure 4.4-3 Temperature dependence of the count rate at several discrimination levels.

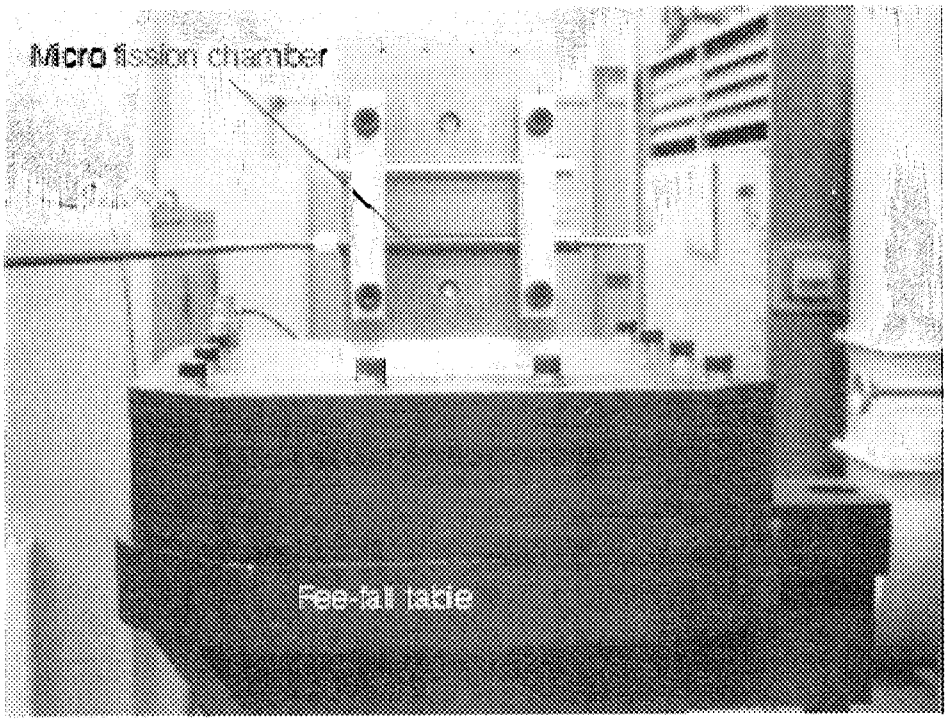

Figure 4.5-1 Picture of the acceleration test by mechanical shocks.

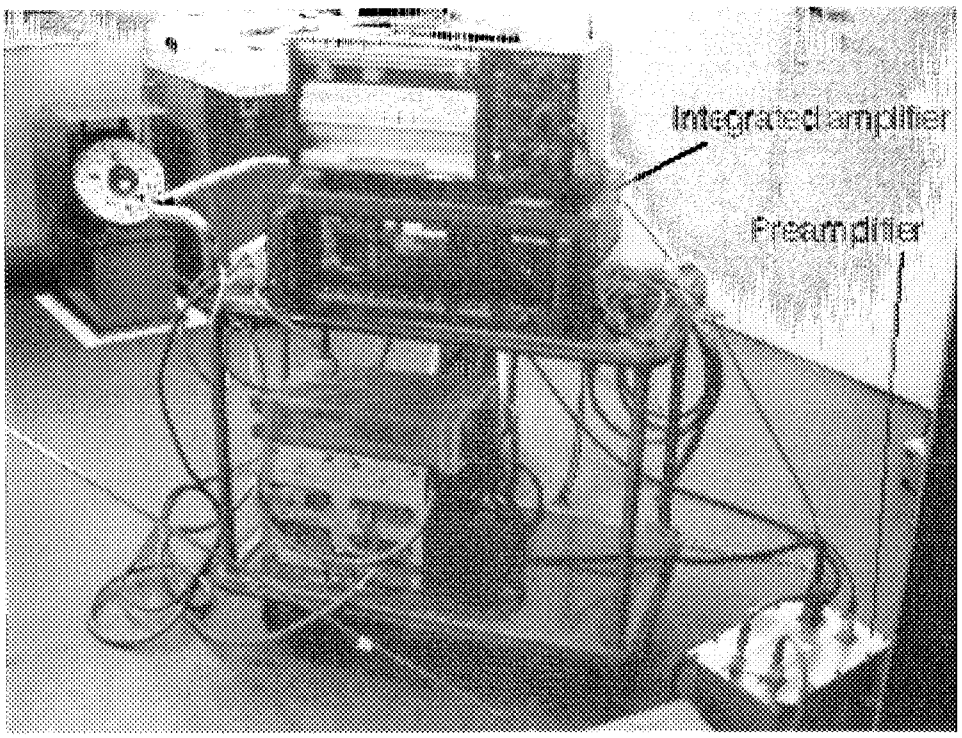

Figure 4.5-2 Picture of the experimental setup for the acceleration test.

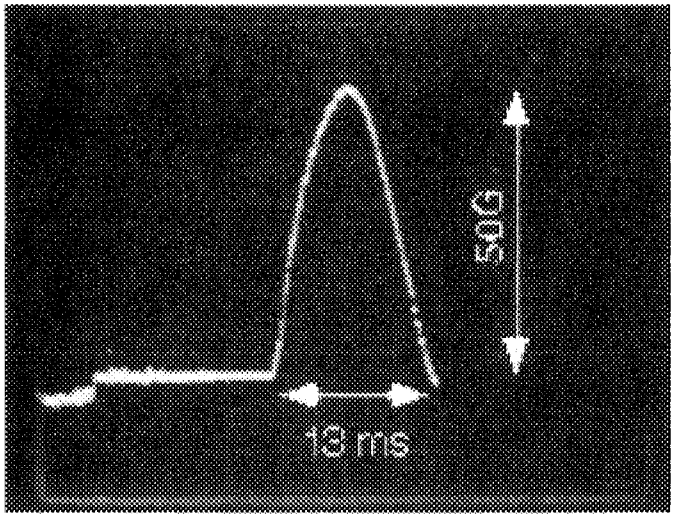

Figure 4.5-3. Waveform of the acceleration.

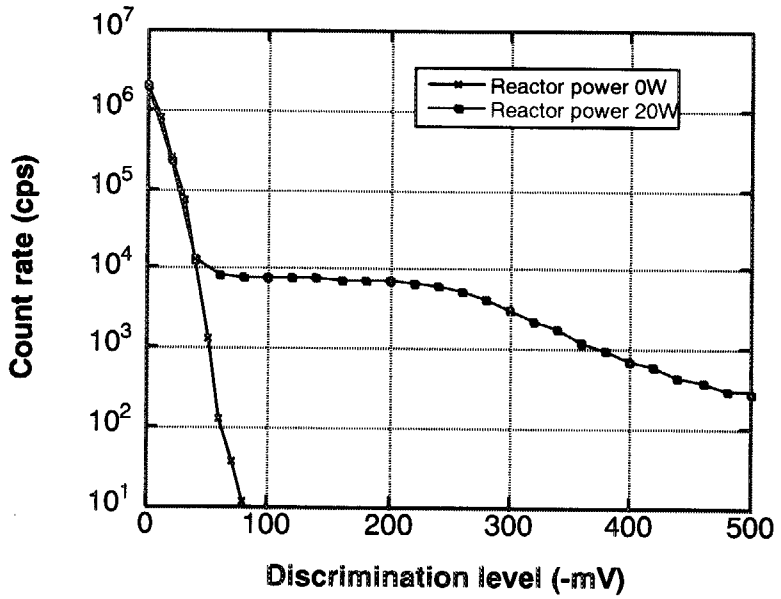

Figure 4.6-1 Discrimination characteristics for thermal neutrons.

5. GAMMA-RAY IRRADIATION TEST

5.1 Test Facility

The dummy chamber was irradiated at the ^{60}Co gamma-ray irradiation facility of JAERI Takasaki. The irradiation facility is shown in Figure 5.1-1. The ^{60}Co gamma-ray source with an intensity of 115 kCi (4286 TBq) is stored in a water pool. The source is lifted into the irradiation room. The irradiation room is shielded with 1.3 m-thick heavy concrete walls. The MI cable of the dummy chamber passed through the shielding wall via a penetration hole. The dummy chamber was put near the gamma-ray source as shown in Figure 5.1-2. The gamma-ray dose rate was 4.7Gy/s at the dummy chamber location, which is almost the equivalent dose rate between the shielding blanket module and the vacuum vessel in ITER, where the micro fission chambers will be installed. The dummy chamber was irradiated for 19.1 hours, which resulted in the total dose of 0.32 MGy.

5.2 Experimental Setup

The block diagram of the electronics for the gamma-ray irradiation test is shown in Figures 5.2-1 and 5.2-2. The analog output of the Campbelling amplifier was measured by a digital voltmeter. The output current of the high voltage power supply was monitored with an ammeter as a current mode measurement. It is expressed by the following equation.

$$I = r\,Q$$

where, I : output current,
r : signal rates,
Q : total electrical charge per incident particle.

On the other hand, the Campbelling output voltage is expressed as follows.

$$V \propto \sqrt{<\sigma^2(t)>}$$

$$<\sigma^2(t)> = \frac{rQ^2}{T}$$

where, V : Campbelling output voltage,
$<\sigma^2(t)>$: variance of current fluctuation,
T : effective measurement time.

Therefore, it should be noticed that the square of Campbelling output is proportional to the signal rates.

5.3 Gamma-ray Sensitivity

Figure 5.3-1 shows the output current of a current mode measurement as a function of bias voltage. The curve is nearly flat above 100 V, which suggests the appropriate bias voltage for in-vessel monitoring is in that range. At the bias voltage of 200 V, the gamma-ray sensitivity is,

$$(4.8\ \mu A)/(1.7 MR/h) = 2.8\ \mu A/(MR/h).$$

Figure 5.3-2 shows the output voltage obtained by the Campbelling mode for several amplifier gains. In case of low gain of 2.875, the effects of gamma-ray irradiation are hardly observed compared with the curve of no irradiation. The difference is not large in case of a medium gain of 28.75 either. On the other hand, with a high gain of 90.75 conspicuously large sensitivity for gamma-rays is observed. Thus a high gain for the amplifier and a bias voltage above 100 V are necessary for monitoring. By comparing the sensitivity with that for neutrons to be described in Section 6, gamma-ray sensitivity in Campbelling mode is equivalent to the neutron count rate of 3×10^5 counts/s for gamma-ray dose of 1 MR/h.

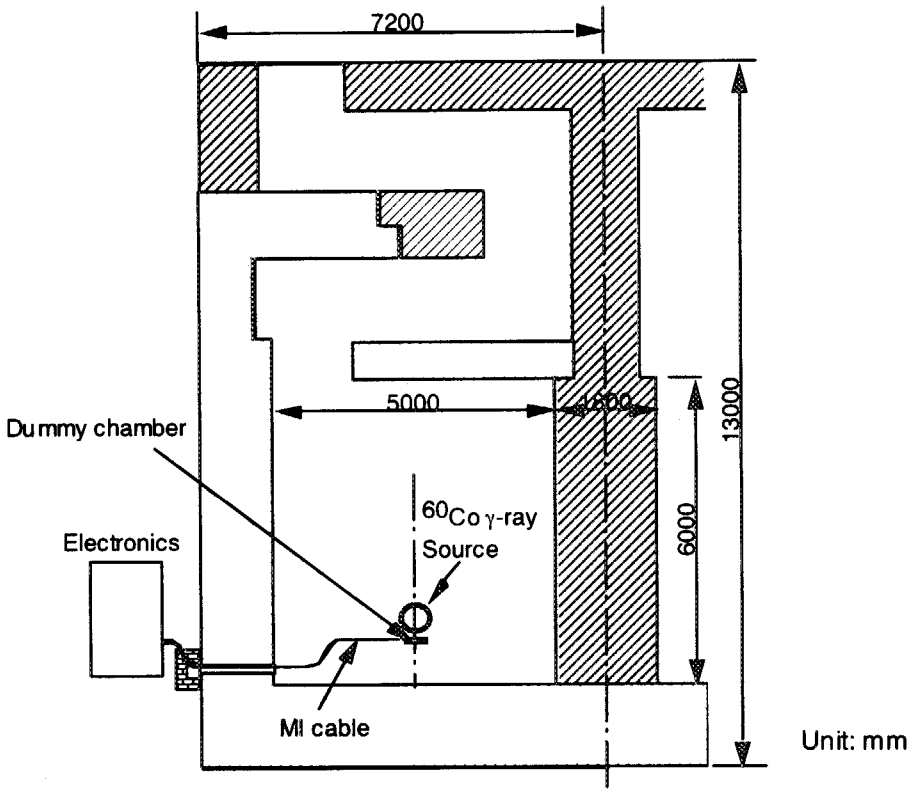

Figure 5.1-1 Schematic view of the ^{60}Co gamma-ray irradiation facility at JAERI TAKASAKI.

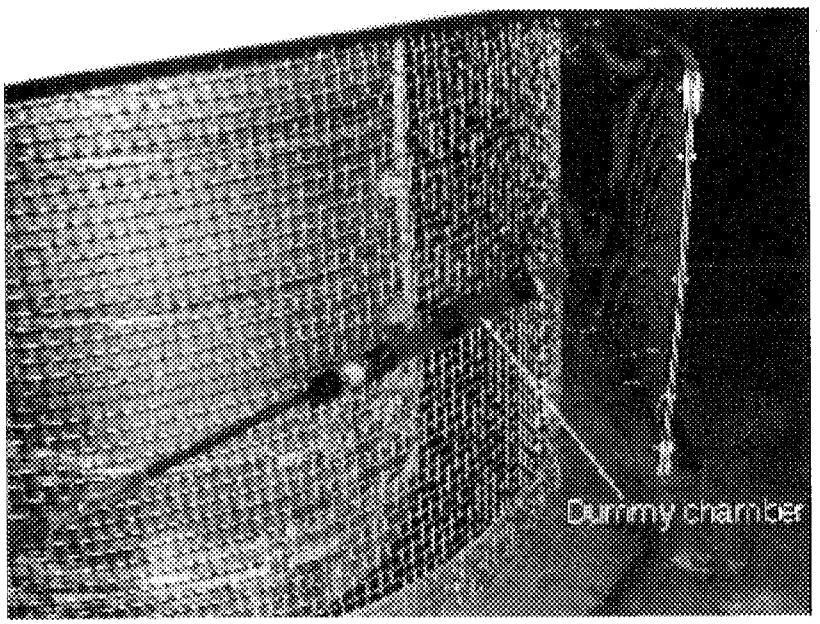

Figure 5.1-2 Picture of the ^{60}Co gamma-ray irradiation facility at JAERI TAKASAKI.

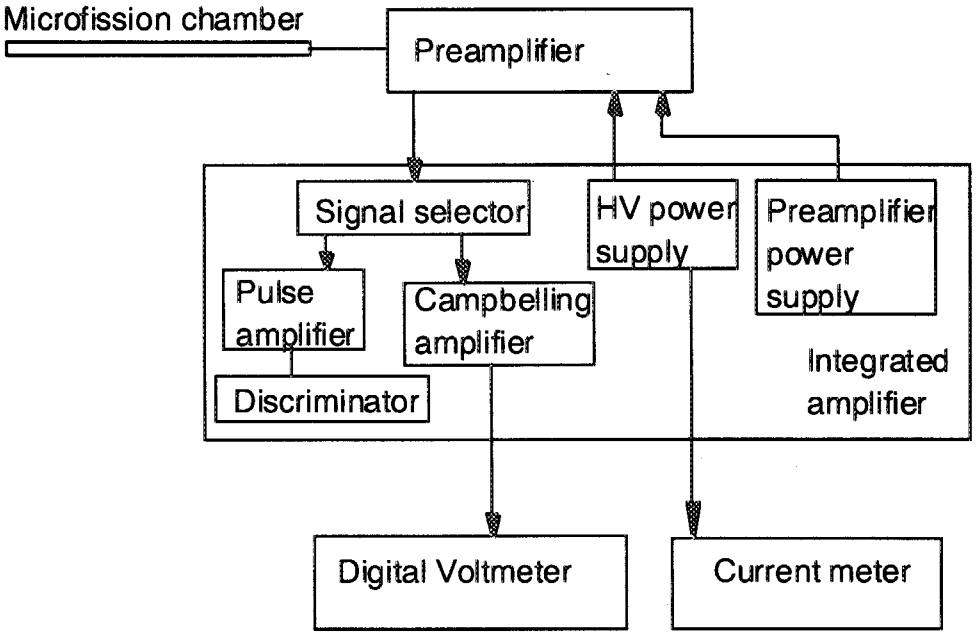

Figure 5.2-1 Experimental setup for the ^{60}Co gamma-ray irradiation tests.

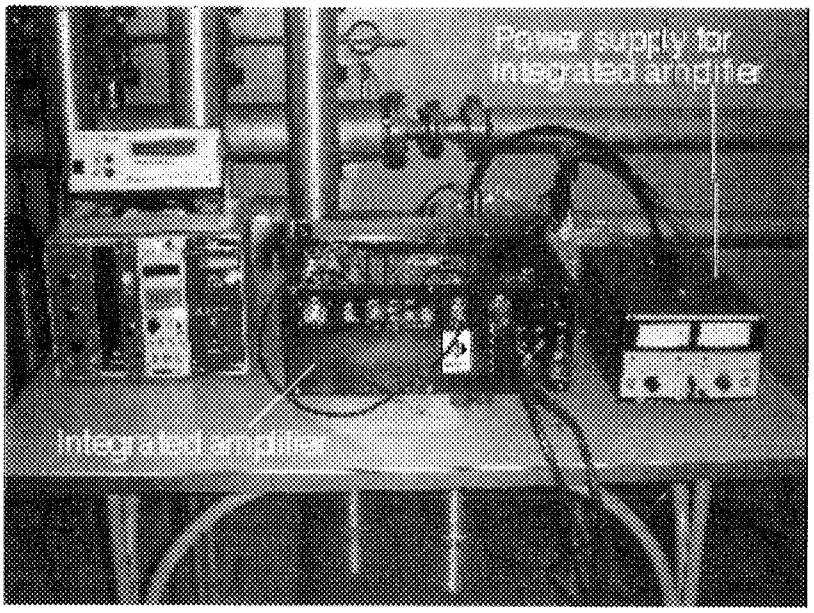

Figure 5.2-2 Picture of the experimental setup for the ^{60}Co gamma-ray irradiation tests.

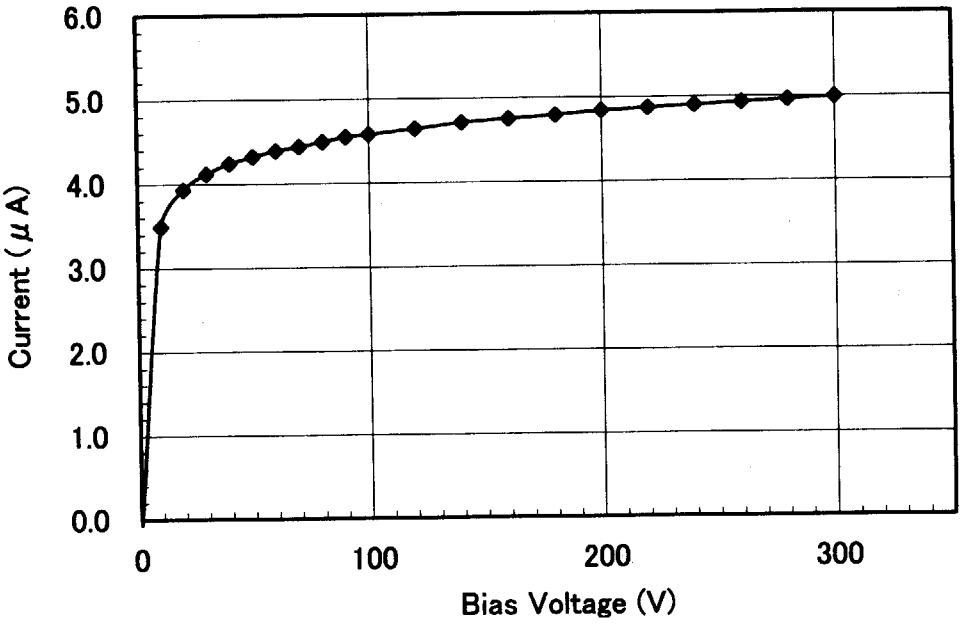

Figure 5.3-1 Current of the dummy chamber for gamma-ray irradiation as a function of bias voltage.

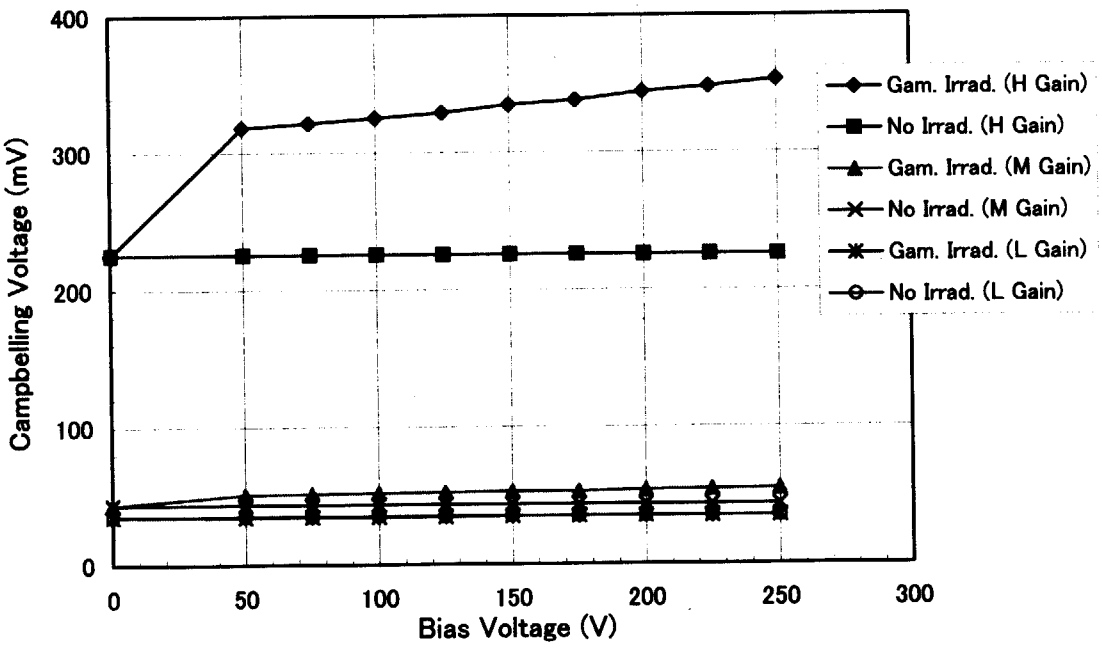

Figure 5.3-2 Campbelling voltage of the dummy chamber for gamma-ray irradiation as a function of bias voltage.

6. PERFORMANCE TESTS UNDER 14 MEV NEUTRONS

6.1 Test Facility

The performance tests under 14 MeV neutrons were performed at Fusion Neutronics Source (FNS) of JAERI Tokai. FNS generates neutrons by D-T reactions using a 350keV deuteron accelerator. A bird's eye view of FNS is shown in Figure 6.1-1. FNS has two target rooms, one houses the target of 80° beam line and the other does that of 0° beam line. In the 1st target room, a beam current up to 3 mA bombards a tritium-titanium target with 0.37 TBq tritium. It produces 14 MeV neutrons up to 3×10^{11} n/s. The second target room has a large rotating target with 37 TBq of tritium, which produces 14 MeV neutrons up to 4×10^{12} n/s with a beam current of 40 mA. In this experiment, the 1st target room was used.

6.2 Experimental Setup

For the sensitivity and linearity measurements, the micro fission chamber and the dummy chamber were located just in front of the target as shown in Figures 6.2-1 and 6.2-2. Both chambers were heated by a ribbon heater from R.T to 250°C. The block diagram of the electronics is shown in Figure 6.2-3. The pulse height distributions were measured with the multi channel analyzer. The pulse output was counted with a discrimination level of -150 mV. Also the output voltage of the Campbelling amplifier and the output current of the high voltage power supply were monitored.

For the measurements for the effects of the surrounding materials, the micro fission chamber was inserted into the mock-up shielding blanket as shown in Figures 6.2-4 and 6.2-5. Here, the pulse height distribution and the counting rate were measured.

6.3 Neutron Sensitivity and Linearity

The pulse height distributions of the micro-fission chamber and the dummy chamber are shown in Fig.6.3-1. A shift of the peak position was observed as the temperature of the chamber was changed. It is necessary to set the discrimination level so as to minimize the influence of the peak shift, however in the present study a temperature-dependent result was obtained. Figure 6.3-2 shows the cumulative pulse number distributions from the largest. If

the discrimination level is above 40, the count rates by micro-fission chamber at high temperature will be about twice larger than those at room temperature according to the figure.

The relation between pulse count rates of the micro-fission chamber and those of alpha counters are shown in Fig.6.3-3 (logarithmic scale) and in Fig.6.3-4 (linear scale). It should be noted that the alpha particle is a fragment of a fusion reaction, and the number of the particle coincides with generated neutrons. An excellent linearity is observed in both figures. The ratios are shown as a function of the beam current in Fig.6.3-5. They are nearly constant as to the current, however, a large discrepancy is observed between curves for different temperatures. The temperature-dependent curve is shown in Fig.6.3-6. The dependency must have been caused by the peak shift in the pulse height distribution.

The relation between the squares of the Campbelling voltages and the count rates of alpha counters are shown in Fig.6.3-7 (logarithmic scale) and in Fig.6.3-8 (linear scale). An excellent linearity is observed up to the neutron yield of about 3×10^{13} counts per 100 second measured by alpha monitor. The ratios of the squared voltages and α counts are shown in Fig.6.3-9. The ratios are nearly constant except when the beam current is very small. However, different curves were also obtained in this case depending on the temperature. Figure 6.3-10 shows the temperature dependency of the squared voltages and α counts ratios. The dependency must have been caused for the same reason as that for fission pulse and α count ratios.

In Figs.6.3-11 and 6.3-12, the relation between the squares of Campbelling voltages and pulse count rates by the micro-fission chamber is shown. An excellent linearity between both operation modes is observed above 10^6 pulse counts of the chamber.

The 14 MeV neutron flux at the chamber position from a unit source in space was estimated to be 3.3×10^{-3} n/cm^2/sec/source. The overall fission rate for the present chamber was calculated to be 1.72×10^{-7} reactions/sec/source at the neutron flux with 2.06 barns (^{235}U) and 1.14 barns (^{238}U) for fission reactions. The efficiency of the chamber was defined as the ratio of measured count rate and the neutron flux. Values are summarized below.

Temperature (°C)	Measured Count Rate/Source	Ratio of Fission Reactions (Meas./Calc.)	Efficiency to Neutron Flux
17	8.02×10^{-8}	0.466	2.42×10^{-5}
250	1.51×10^{-7}	0.880	4.56×10^{-5}

When the temperature is 250 °C, the count rate attains nearly 90% of the estimated value, and the efficiency for 14 MeV neutrons is 4.56×10^{-5}.

6.4 Effects of the surrounding materials

The pulse height distributions of the micro-fission chamber inserted into the mock-up shielding blanket are shown in Fig.6.3-13. They show similar shapes above noise level. The only difference is the number of counts. It shows that neutron spectra are similar and electronics condition for the measurement is common at all 4 positions.

In order to estimate the efficiency of the micro-fission chamber, a Monte Calro calculation was performed for the geometry shown in Fig.6.2-4 with MCNP code. Calculational results are shown with measured count rates in Fig.6.3-14. All values were normalized to unit source intensity. Fission reaction rates were integrated over the total amount of fissile material of a chamber.

Both measured and calculated fission reaction rates are well consistent in Fig.6.3-14. The C/E values are shown in Fig.6.3-15. Although the calculated reaction rate is about 40% larger than the measured value at the front surface of the mock-up geometry (Position 1), the differences are merely 10% at the other positions. The agreement shows the present micro-fission chamber is very effective to catch neutrons at detector positions.

In Fig.6.3-14, the measured fission reaction rate (count rate) is 3.6×10^{-4} times the total neutron flux, and 2.4×10^{-3} times the fast neutron flux above 10 MeV at the front surface of the mock-up geometry (Position 1). The values mean efficiencies of the chamber to total and 14 MeV neutron fluxes.

In Fig.6.3-16, neutron fluxes and reaction rates normalized at the front surface are shown. As the position becomes deeper from the front surface, the calculated reaction rate and total flux decrease roughly as much as the measured reaction rate, however the 14 MeV neutron flux decreases more steeply. It is because the fast neutron flux does not include much of a reflected component, while the fission count rate does. Therefore the efficiency of the chamber for 14 MeV neutron flux becomes larger under the influence of the surrounding material.

In Fig.6.3-17, calculated neutron spectra at 4 positions are shown. The shapes are nearly similar to one another except for the 14 MeV neutron peak. The peak becomes smaller as the position becomes deeper from the front surface due to the fore-mentioned reason.

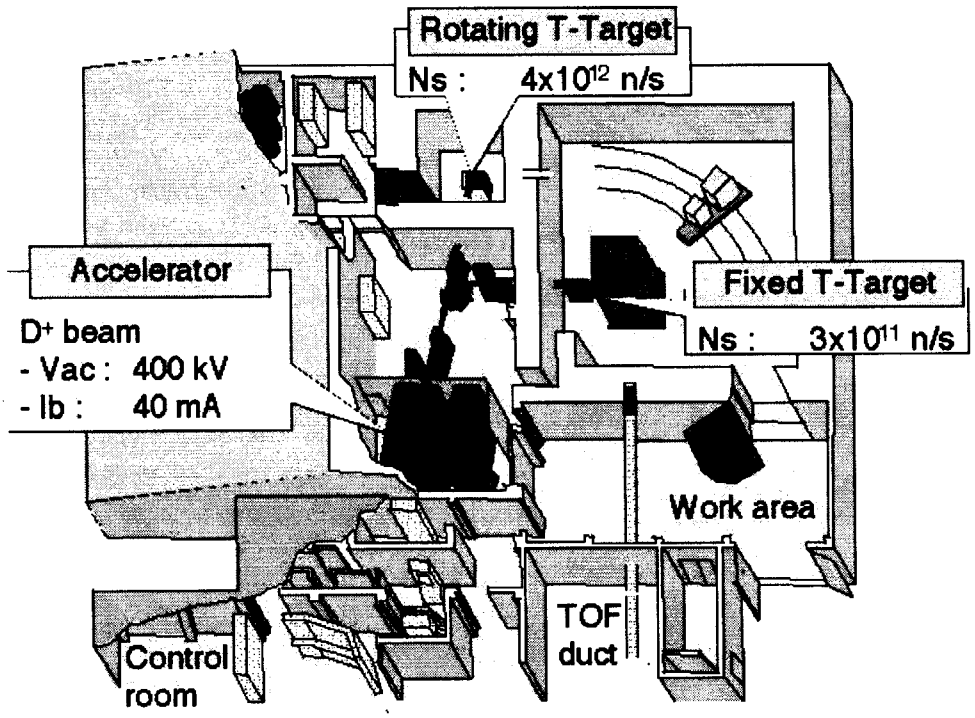

Figure 6.1-1 Bird's eye view of FNS.

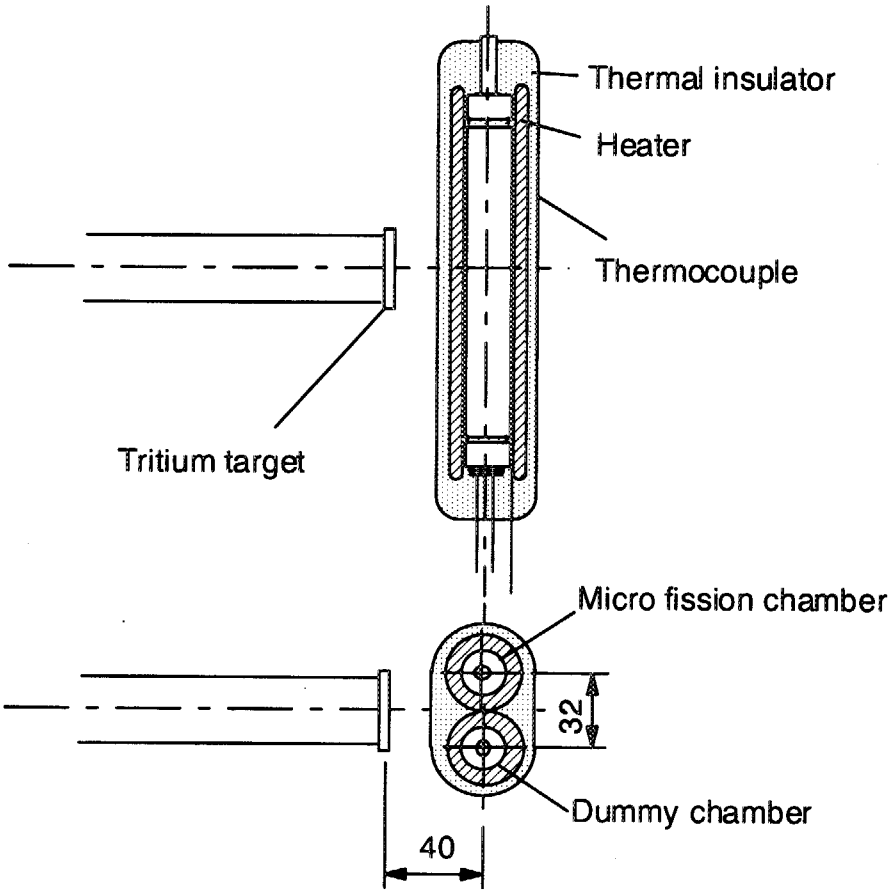

Figure 6.2-1 Experimental setup for the sensitivity and linearity measurements.

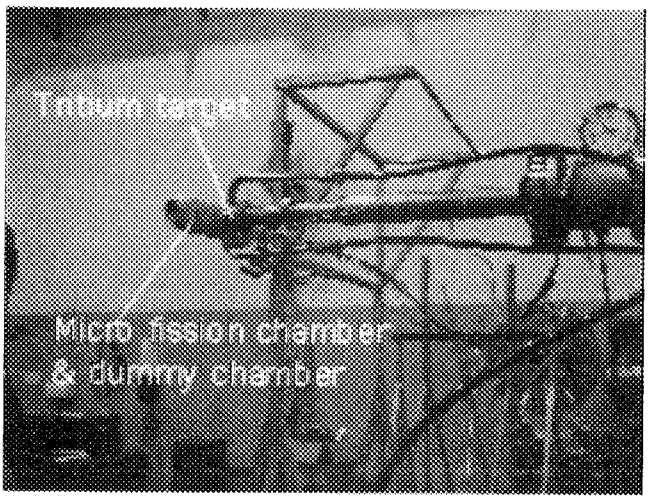

Figure 6.2-2 Picture of the experimental setup for the sensitivity and linearity measurements.

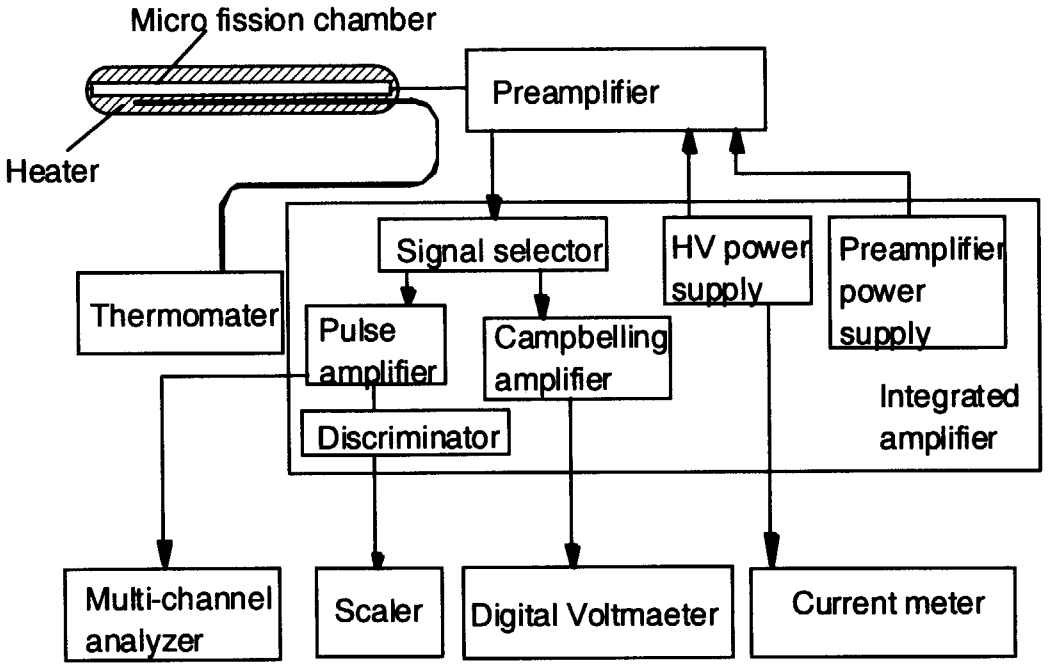

Figure 6.2-3 Block diagram of the electronics for the sensitivity and linearity measurements.

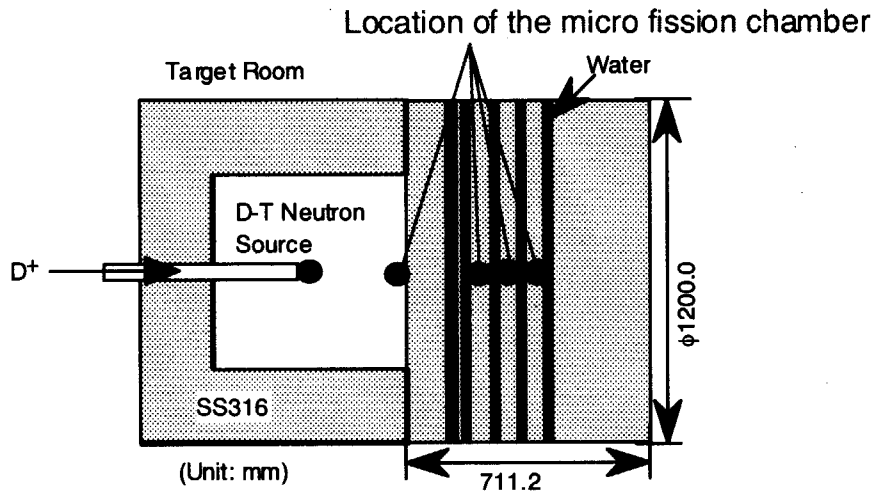

Figure 6.2-4 Experimental setup of the measurements for the effects of the surrounding materials.

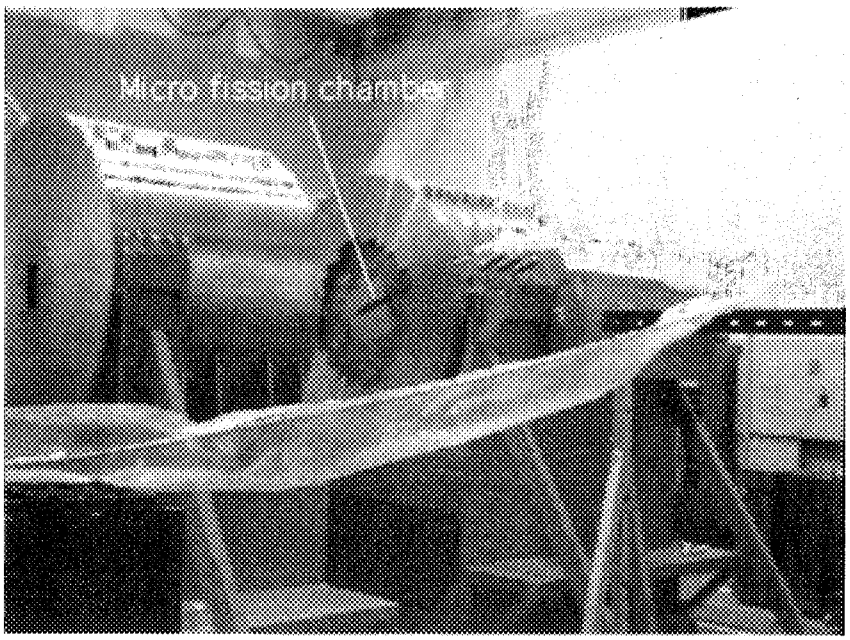

Figure 6.2-5 Picture of the experimental setup of the measurements for the effects of the surrounding materials.

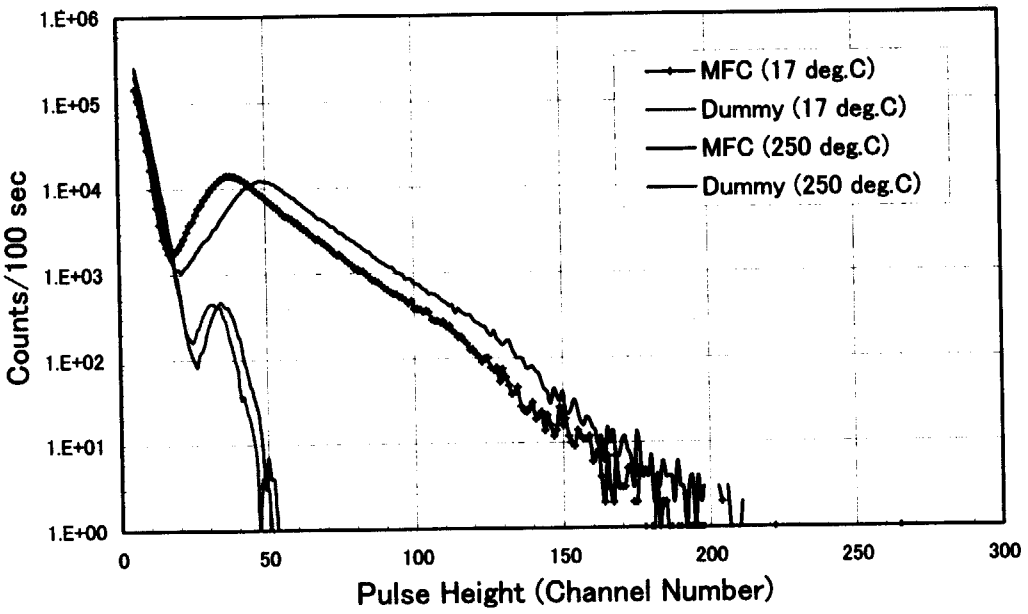

Figure 6.3-1 Pulse height distributions of the microfission chamber and the dummy chamber.

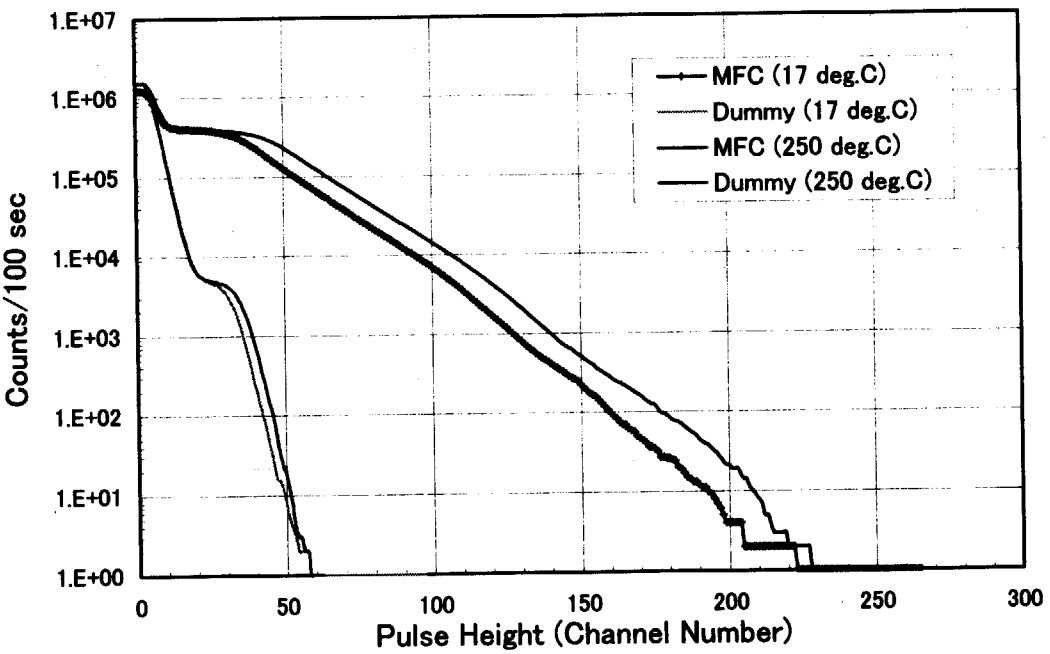

Figure 6.3-2 Cumulative pulse height distributions of the microfission chamber and the dummy chamber.

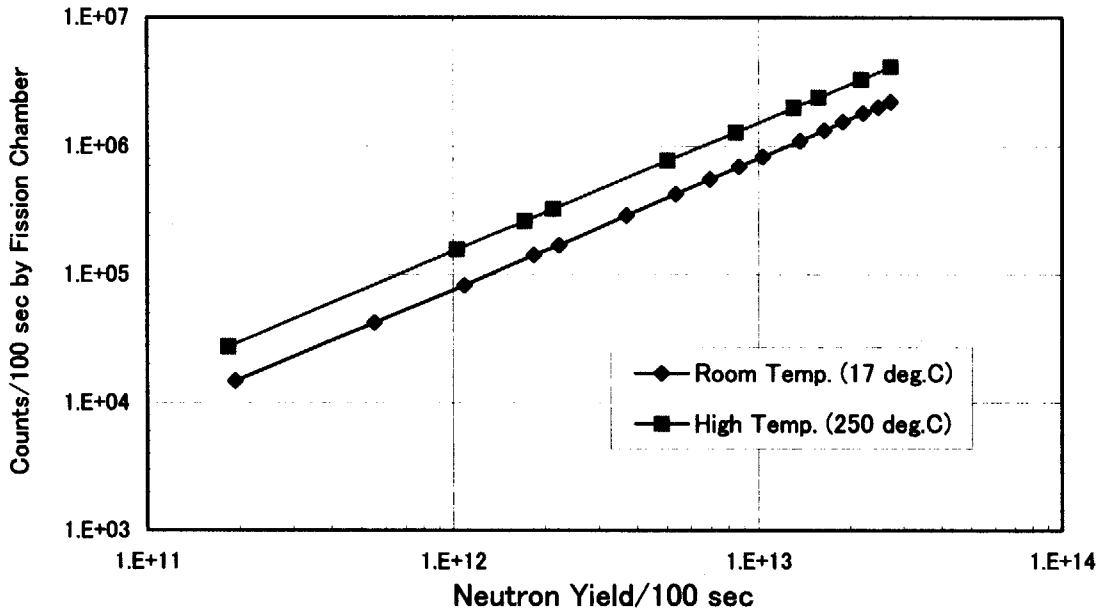

Figure 6.3-3 Linearity between counts by the microfission chamber and neutron yield by the α monitor (logarithmic scale).

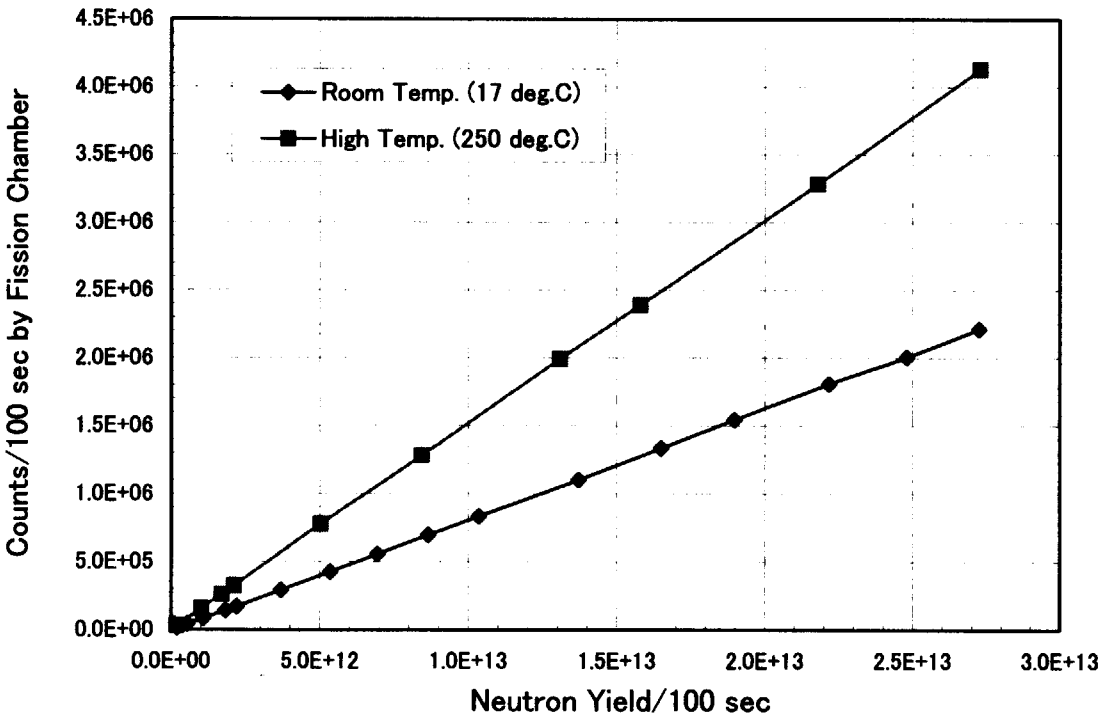

Figure 6.3-4 Linearity between counts by the microfission chamber and neutron yield by the α monitor (linear scale).

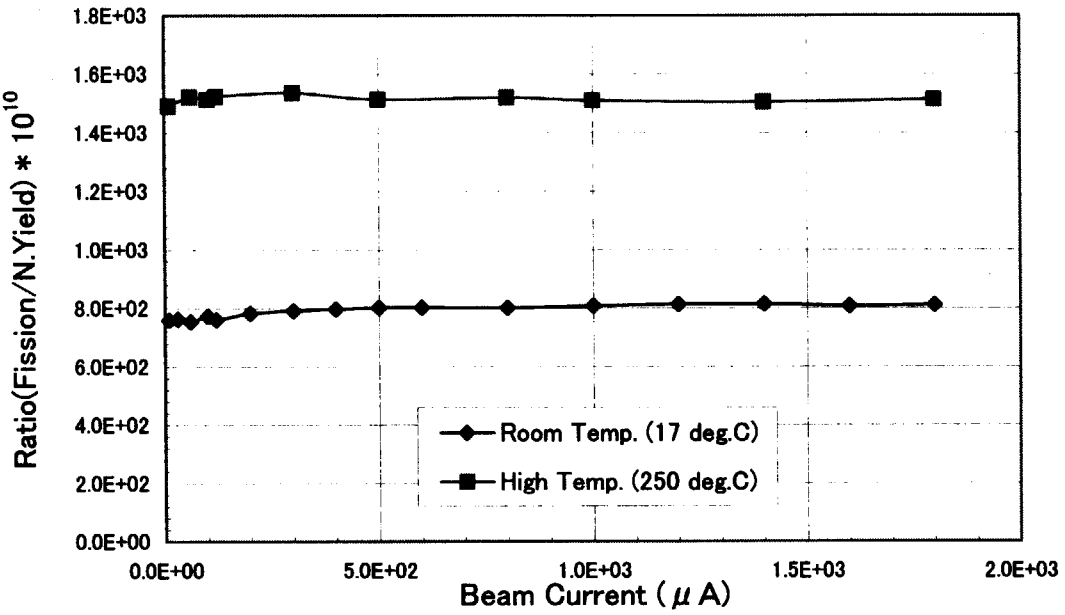

Figure 6.3-5 Ratios of fission counts to neutron yield as a function of beam current.

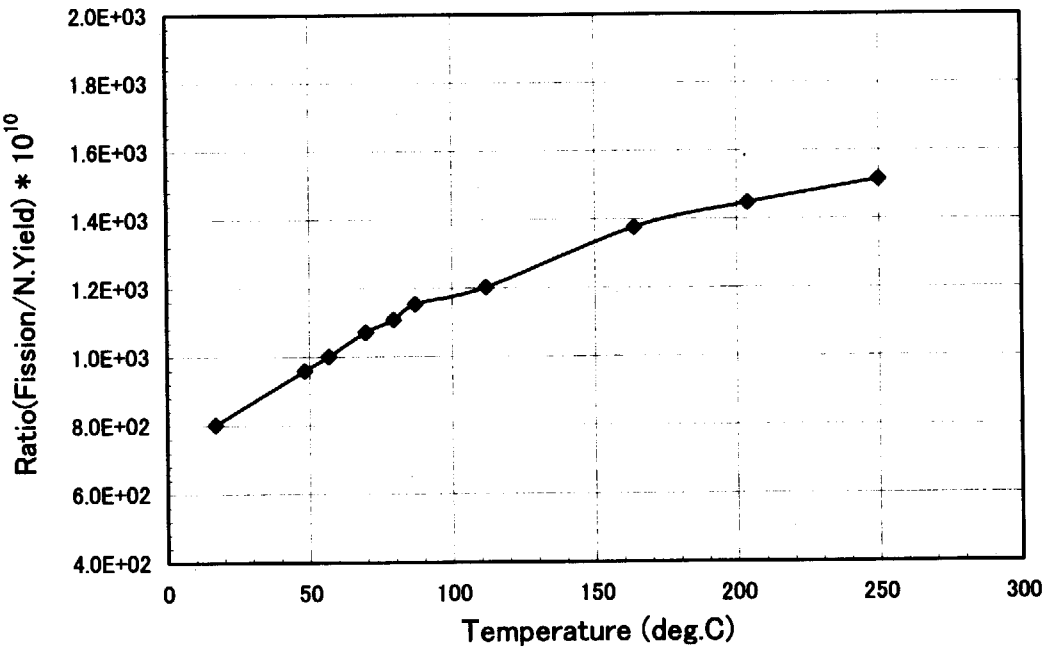

Figure 6.3-6 Ratios of fission counts to neutron yield as a function of temperature.

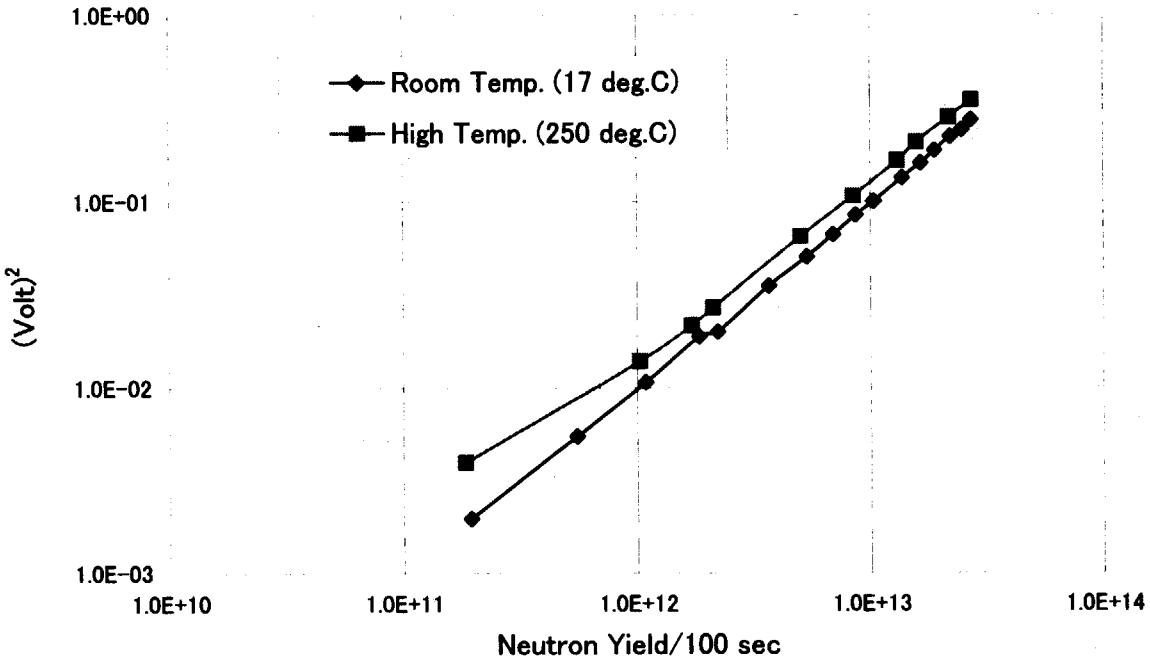

Figure 6.3-7 Linearity between square voltage and neutron yield by the α monitor (logarithmic scale).

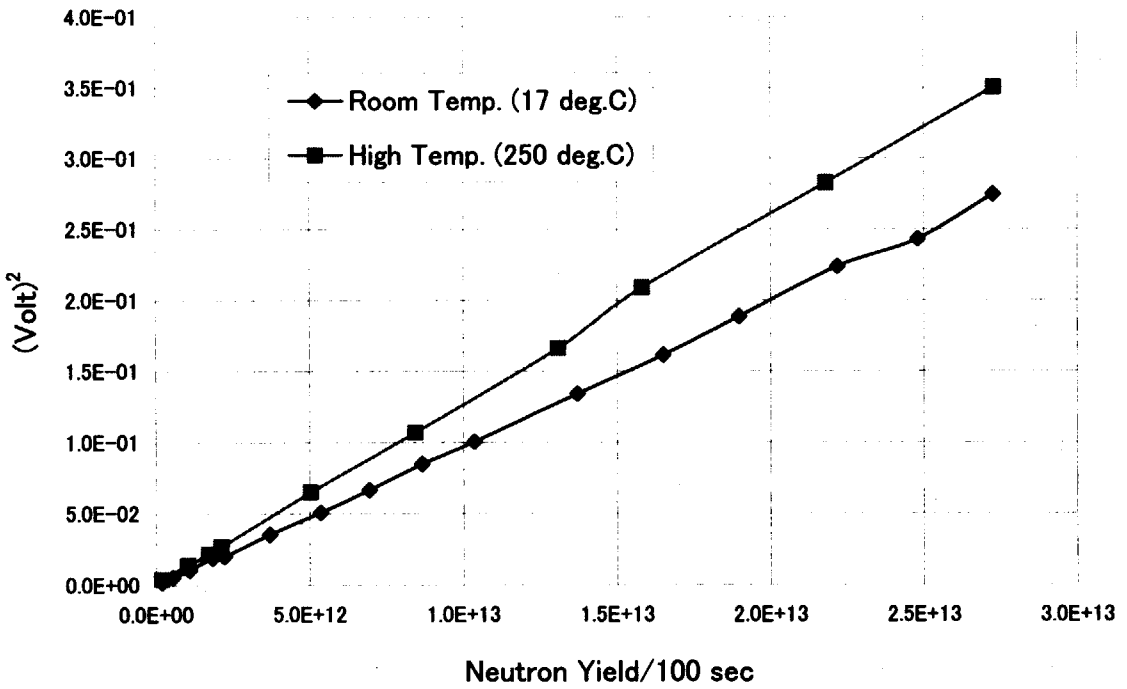

Figure 6.3-8 Linearity between square voltage and neutron yield by the α monitor (linear scale).

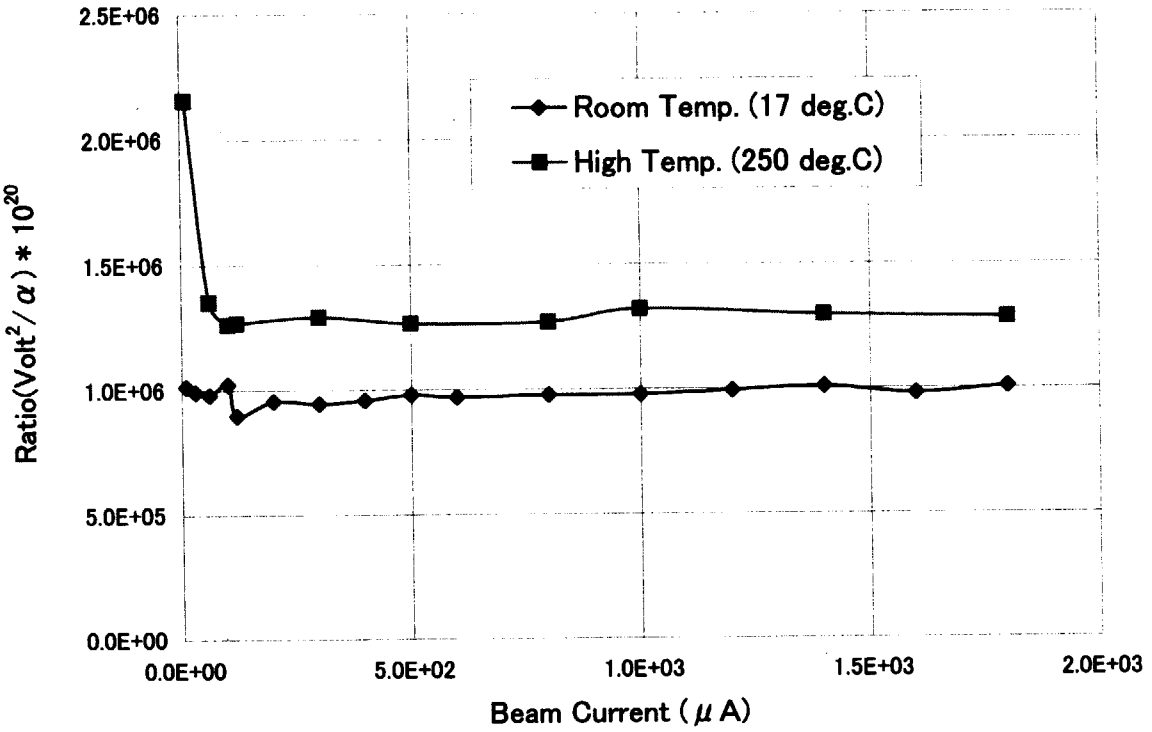

Figure 6.3-9 Ratios of square Campbelling voltage to neutron yield as a function of beam current

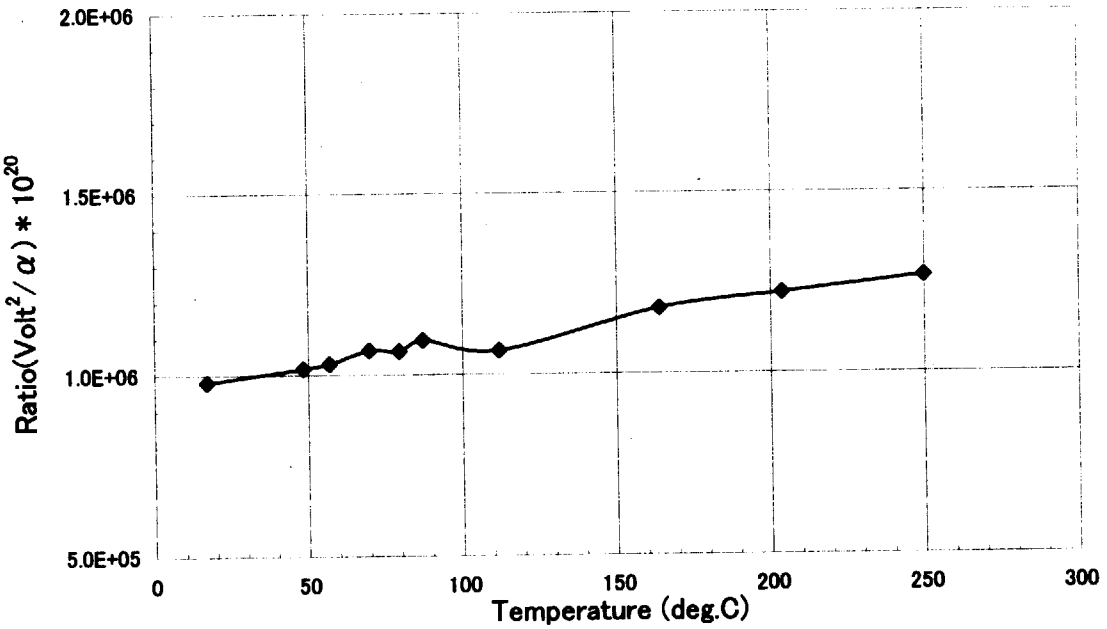

Figure 6.3-10 Ratios of square Campbelling voltage to neutron yield as a function of temperature

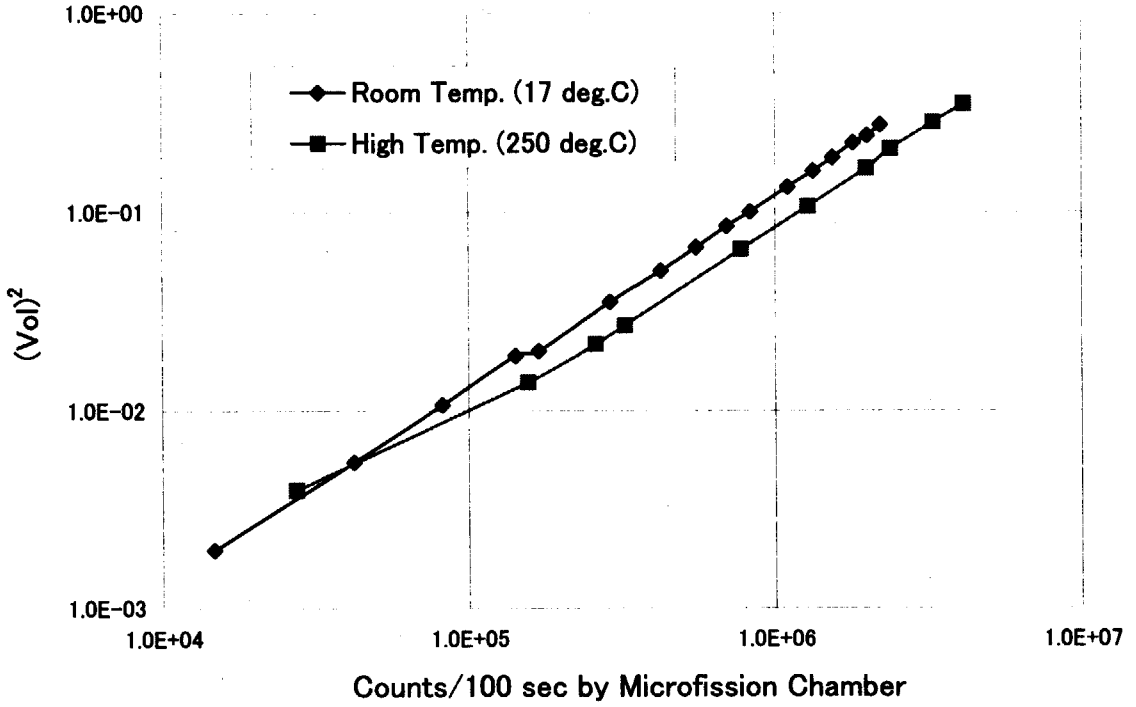

Figure 6.3-11 Linearity between square voltage and counts by the microfission chamber

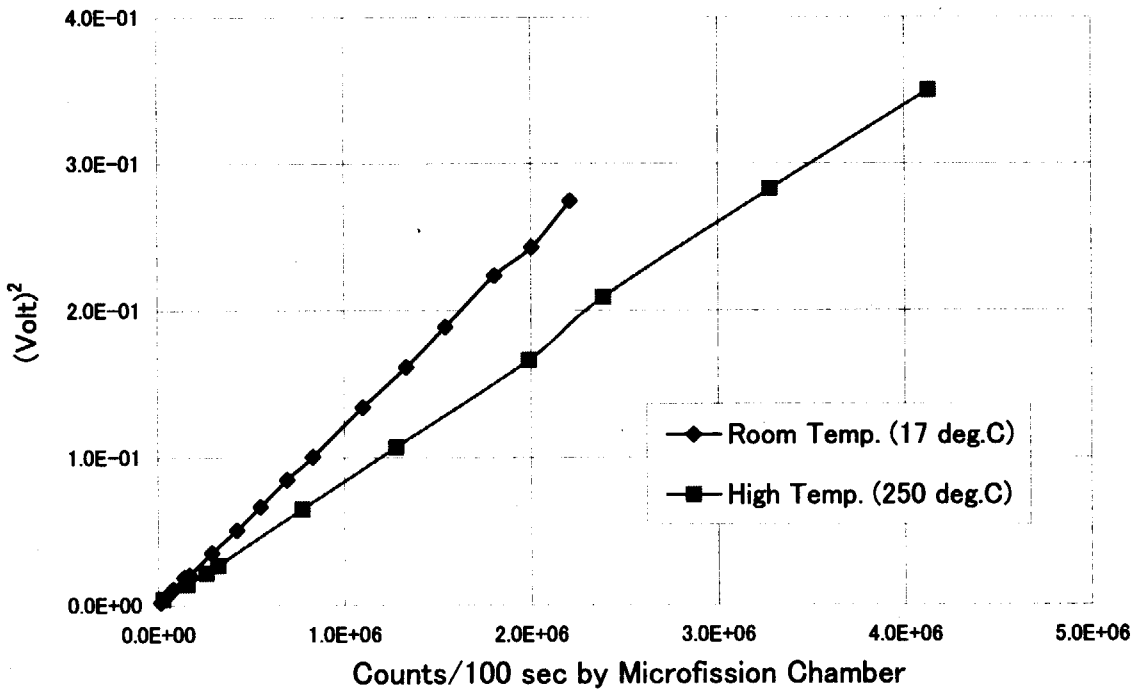

Figure 6.3-12 Linearity between square voltage and counts by the microfission chamber

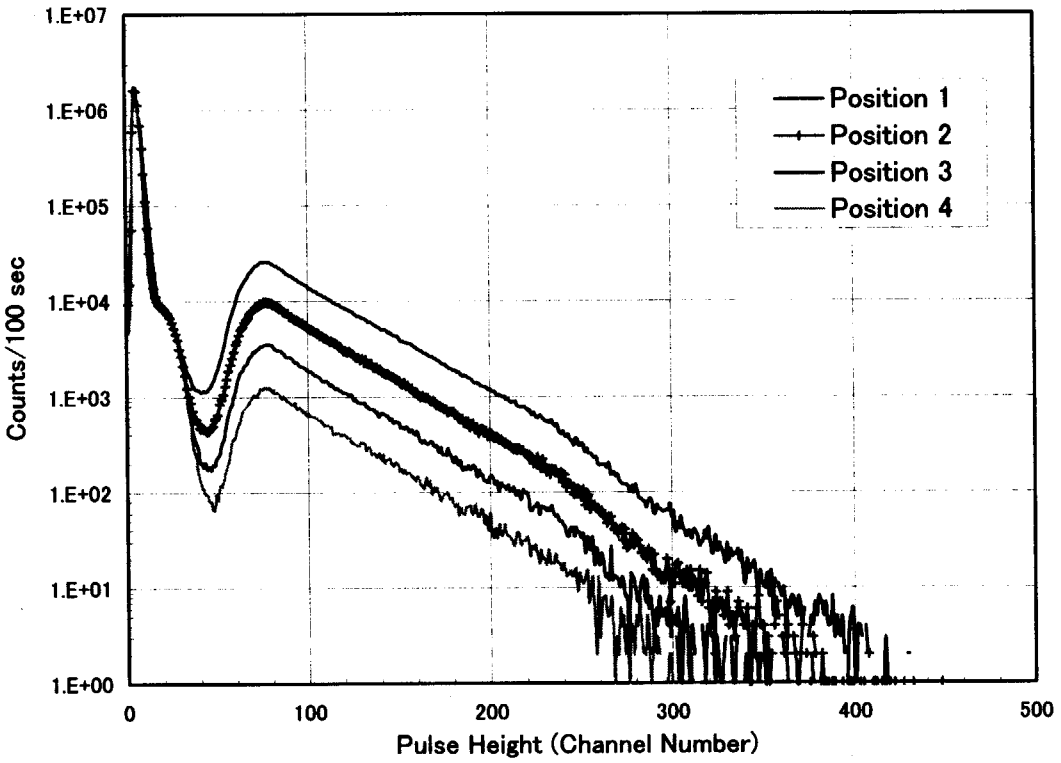

Figure 6.3-13 Pulse height distributions of the microfission chamber in shielding materials.

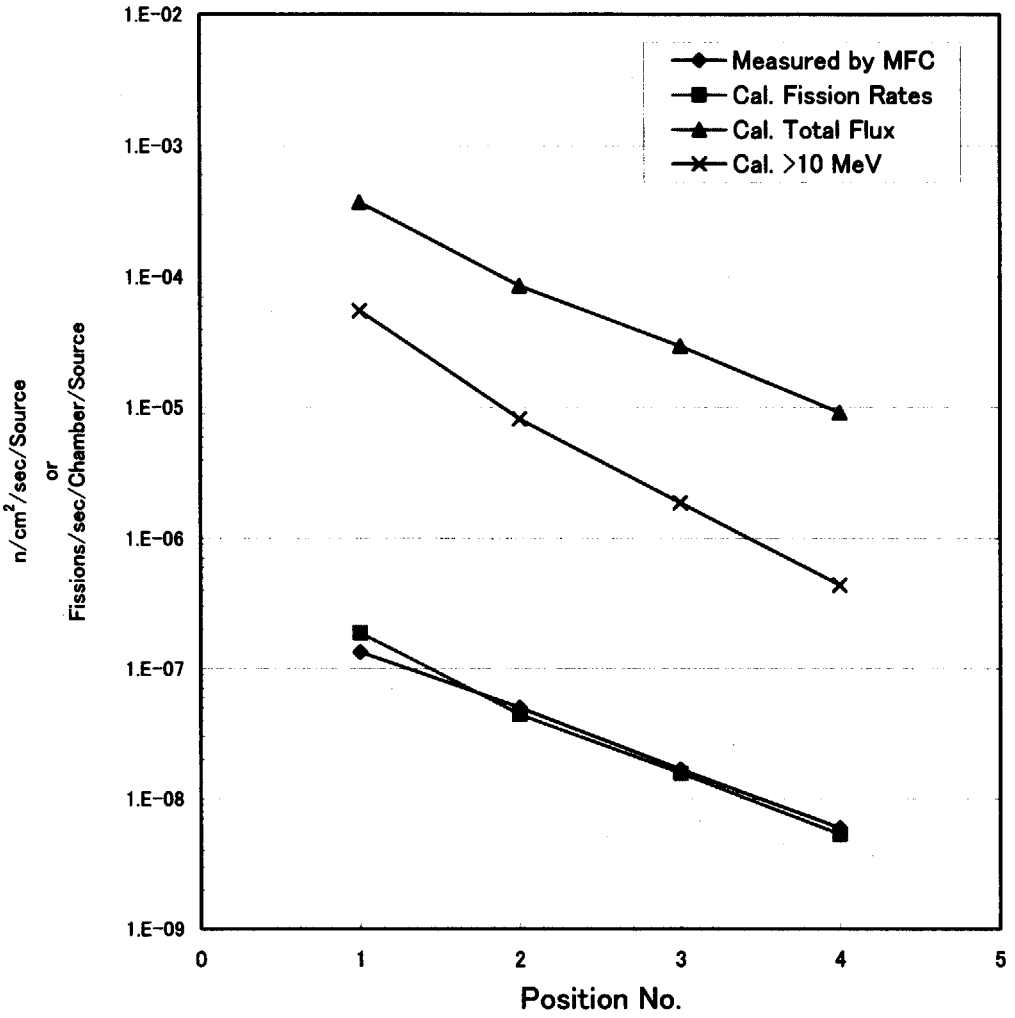

Figure 6.3-14 Comparison of measured and calculated fission rates for the microfission chamber.

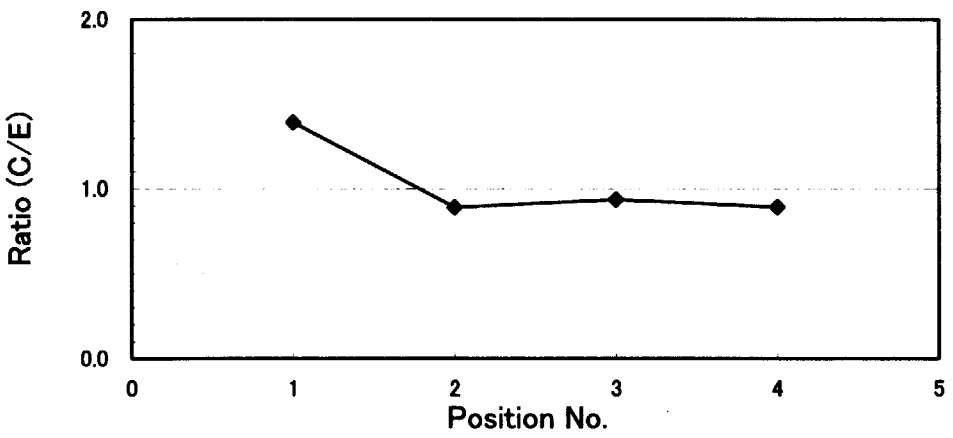

Figure 6.3-15 Ratios of calculated to experimental fission rates for the microfission chamber.

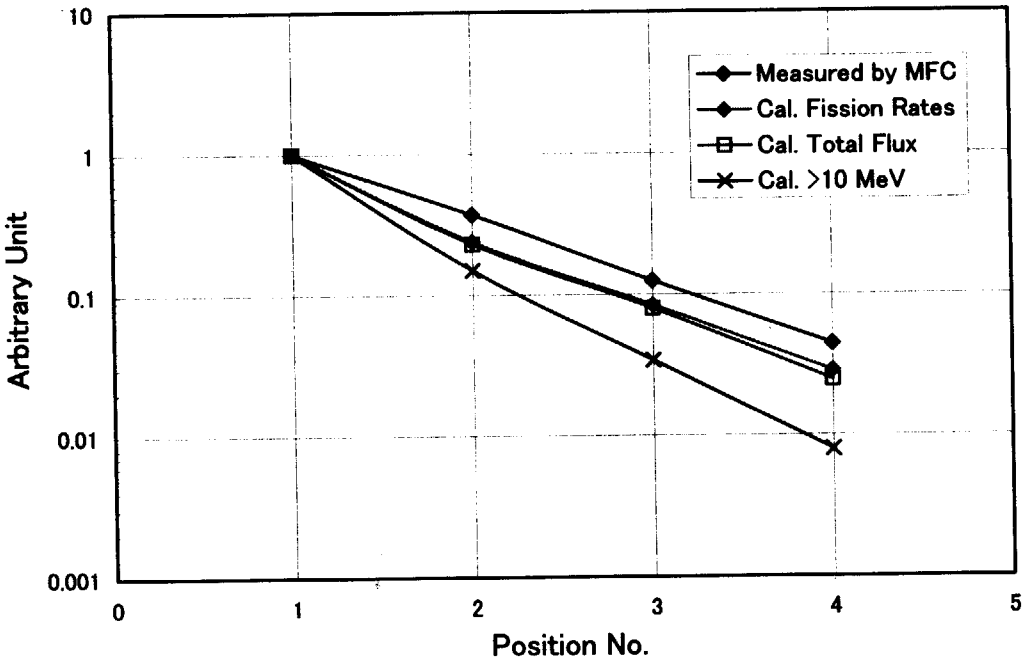

Figure 6.3-16 Comparison of mesured and calculated values normalized at position 1 in the shielding material.

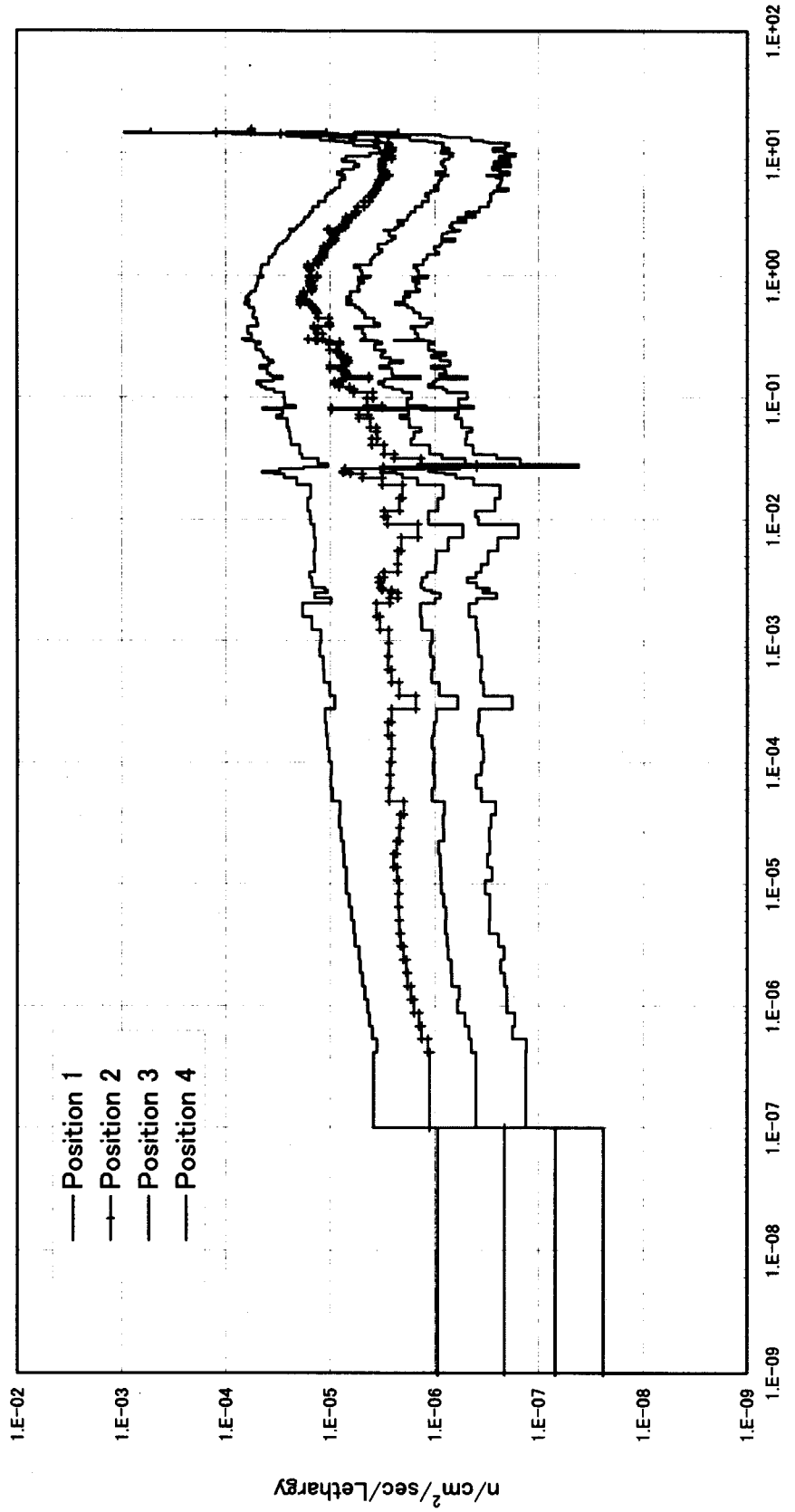

Figure 6.3-17 Neutron spectrum calculated by MCNP code in the shielding material.

7. CONCLUSION

A micro fission chamber with 12 mg UO_2 and a dummy chamber without uranium were fabricated for the in-vessel neutron flux monitor of ITER-FEAT. These detectors are filled with 14.6 atm of Ar + 5% N_2 gas, which enable the pulse counting and Campbelling mode. The dimensional check shows that those detectors were fabricated within the permitted dimensional error. The dummy chamber with MI cable was tested for vacuum leaks at room temperature. We confirmed that the He leak rate was less than the detection limit, 1×10^{-8} cc/s. The resistance between the center conductor and the outer sheath was measured in the temperature range from room temperature (20°C) to 350°C with an impedance analyser. The measured resistances were within the acceptable range for the micro fission chamber performance. An acceleration test was carried out by 10 times of mechanical shocks with 50G. The induced count rate was negligibly small and there was no change in the Campbelling output signal. The gamma-ray sensitivity was measured for the dummy chamber using the ^{60}Co gamma-ray irradiation facility of JAERI Takasaki. We confirmed that the output signal of the Campbelling mode by gamma-rays would be less than 0.1 % of that by neutrons behind the blanket module in ITER-FEAT. The detector performance for 14 MeV neutrons was investigated by using the FNS facility. Excellent linearity of the count rate versus the neutron flux was confirmed in the temperature range from 20°C to 250°. However, a positive temperature dependence of the sensitivity for 14 MeV neutrons was recognized, which might be caused by the increase in the pulse height with temperature. Effects of the change of surrounding materials were evaluated by sensitivity measurements of the micro fission chamber inserted into the shielding blanket mock-up. The sensitivity was enhanced by the slow-downed neutrons, which agreed with a calculation using MCNP-4C code.

Finally, we can conclude that the developed micro fission chamber is applicable for ITER-FEAT.

ACNOWLEDGMENTS

The authors would like to express their gratitude to the operating staff of FNS and people of the ^{60}Co irradiation facility for their operation of those facilities. This report has been prepared as an account of work assigned to the Japanese Home Team under Task Agreement number N 55 TT 07 FJ within the Agreement among the European Atomic Energy Community, the Government of Japan, and the Government of the Russian Federation on Cooperation in the Engineering Design Activities for the International Thermonuclear Experimental Reactor ("ITER EDA Agreement") under the auspices of the International Atomic Energy Agency (IAEA).

REFERENCES

[1] V.Mukhovatov, H. Hopman, S. Yamamoto, et al., in: ITER Diagnostics, ITER Documantation Series, No.33, IAEA, Vienna (1991).

[2] T. Iguchi, J. Kaneko, M. Nakazawa, T. Matoba, T. Nishitani and S. Yamamoto, Conceptional design of neutron diagnostics system for fusion experimental reactor, Fusion Eng. Design 28: 689 (1995).

[3] T. Nishitani, K. Ebisawa, T. Iguchi and T. Matoba, Design of ITER neutron yield monitor using microfission chambers, Fusion Eng. Design 34-35, 567 (1997).

[4] T. Nishitani, S. Kasai, L.C. Johnson, K. Ebisawa, C. Walker and T. Ando. Neutron monitor using microfission chambers for the International Thermonuclear Fusion Reactor, rev. Sci. Instrum. 70, 1141 (1999).

[5] T. Nishitani, Design of Micro Fission Chambers (WBS 5.5 B.03), Final report for the Design Task D426-J-1, (2001).

[6] T. Nakamura, H. Maekawa, Y. Ikeda and Y. Oyama, A DT Neutron Source for Fusion Neutronics Experiments at the JAERI, Proc. Int. Ion Eng. Congress – ISIAT '83 & IAPT '83, Kyoto, Japan, Vol. 1 pp. 567-570 (1983).

[7] Y. Endo, T. Ito and E. Seki, A counting-Cambelling neutron measurement system and its experimental results by test reactor, IEEE Trans. Nucl. Sci. NS-29: 714 (1982).

This is a blank page.

国際単位系 (SI) と換算表

表 1　SI基本単位および補助単位

量	名称	記号
長さ	メートル	m
質量	キログラム	kg
時間	秒	s
電流	アンペア	A
熱力学温度	ケルビン	K
物質量	モル	mol
光度	カンデラ	cd
平面角	ラジアン	rad
立体角	ステラジアン	sr

表 2　SIと併用される単位

名称	記号
分，時，日	min，h，d
度，分，秒	°，′，″
リットル	l，L
トン	t
電子ボルト	eV
原子質量単位	u

1 eV = 1.60218 × 10^{-19} J

1 u = 1.66054 × 10^{-27} kg

表 5　SI接頭語

倍数	接頭語	記号
10^{18}	エクサ	E
10^{15}	ペタ	P
10^{12}	テラ	T
10^{9}	ギガ	G
10^{6}	メガ	M
10^{3}	キロ	k
10^{2}	ヘクト	h
10^{1}	デカ	da
10^{-1}	デシ	d
10^{-2}	センチ	c
10^{-3}	ミリ	m
10^{-6}	マイクロ	μ
10^{-9}	ナノ	n
10^{-12}	ピコ	p
10^{-15}	フェムト	f
10^{-18}	アト	a

表 3　固有の名称をもつSI組立単位

量	名称	記号	他のSI単位による表現
周波数	ヘルツ	Hz	s^{-1}
力	ニュートン	N	m·kg/s^2
圧力，応力	パスカル	Pa	N/m^2
エネルギー，仕事，熱量	ジュール	J	N·m
工率，放射束	ワット	W	J/s
電気量，電荷	クーロン	C	A·s
電位，電圧，起電力	ボルト	V	W/A
静電容量	ファラド	F	C/V
電気抵抗	オーム	Ω	V/A
コンダクタンス	ジーメンス	S	A/V
磁束	ウェーバ	Wb	V·s
磁束密度	テスラ	T	Wb/m^2
インダクタンス	ヘンリー	H	Wb/A
セルシウス温度	セルシウス度	℃	
光束	ルーメン	lm	cd·sr
照度	ルクス	lx	lm/m^2
放射能	ベクレル	Bq	s^{-1}
吸収線量	グレイ	Gy	J/kg
線量当量	シーベルト	Sv	J/kg

表 4　SIと共に暫定的に維持される単位

名称	記号
オングストローム	Å
バーン	b
バール	bar
ガル	Gal
キュリー	Ci
レントゲン	R
ラド	rad
レム	rem

1 Å = 0.1 nm = 10^{-10} m

1 b = 100 fm^2 = 10^{-28} m^2

1 bar = 0.1 MPa = 10^5 Pa

1 Gal = 1 cm/s^2 = 10^{-2} m/s^2

1 Ci = 3.7 × 10^{10} Bq

1 R = 2.58 × 10^{-4} C/kg

1 rad = 1 cGy = 10^{-2} Gy

1 rem = 1 cSv = 10^{-2} Sv

（注）

1. 表1－5は「国際単位系」第5版，国際度量衡局 1985年刊行による。ただし，1 eVおよび1 uの値はCODATAの1986年推奨値によった。
2. 表4には海里，ノット，アール，ヘクタールも含まれているが日常の単位なのでここでは省略した。
3. barは，JISでは流体の圧力を表わす場合に限り表2のカテゴリーに分類されている。
4. EC閣僚理事会指令ではbar，barnおよび「血圧の単位」mmHgを表2のカテゴリーに入れている。

換　算　表

力	N(=10^5 dyn)	kgf	lbf
	1	0.101972	0.224809
	9.80665	1	2.20462
	4.44822	0.453592	1

粘度　1 Pa·s(N·s/m^2) = 10 P(ポアズ)(g/(cm·s))

動粘度　1 m^2/s = 10^4 St(ストークス)(cm^2/s)

圧力	MPa(=10 bar)	kgf/cm^2	atm	mmHg(Torr)	lbf/in^2(psi)
	1	10.1972	9.86923	7.50062 × 10^3	145.038
	0.0980665	1	0.967841	735.559	14.2233
	0.101325	1.03323	1	760	14.6959
	1.33322 × 10^{-4}	1.35951 × 10^{-3}	1.31579 × 10^{-3}	1	1.93368 × 10^{-2}
	6.89476 × 10^{-3}	7.03070 × 10^{-2}	6.80460 × 10^{-2}	51.7149	1

エネルギー・仕事・熱量	J(=10^7 erg)	kgf·m	kW·h	cal(計量法)	Btu	ft·lbf	eV
	1	0.101972	2.77778 × 10^{-7}	0.238889	9.47813 × 10^{-4}	0.737562	6.24150 × 10^{18}
	9.80665	1	2.72407 × 10^{-6}	2.34270	9.29487 × 10^{-3}	7.23301	6.12082 × 10^{19}
	3.6 × 10^6	3.67098 × 10^5	1	8.59999 × 10^5	3412.13	2.65522 × 10^6	2.24694 × 10^{25}
	4.18605	0.426858	1.16279 × 10^{-6}	1	3.96759 × 10^{-3}	3.08747	2.61272 × 10^{19}
	1055.06	107.586	2.93072 × 10^{-4}	252.042	1	778.172	6.58515 × 10^{21}
	1.35582	0.138255	3.76616 × 10^{-7}	0.323890	1.28506 × 10^{-3}	1	8.46233 × 10^{18}
	1.60218 × 10^{-19}	1.63377 × 10^{-20}	4.45050 × 10^{-26}	3.82743 × 10^{-20}	1.51857 × 10^{-22}	1.18171 × 10^{-19}	1

1 cal = 4.18605 J(計量法)

= 4.184 J　(熱化学)

= 4.1855 J　(15 °C)

= 4.1868 J(国際蒸気表)

仕事率　1 PS(仏馬力)

= 75 kgf·m/s

= 735.499 W

放射能	Bq	Ci
	1	2.70270 × 10^{-11}
	3.7 × 10^{10}	1

吸収線量	Gy	rad
	1	100
	0.01	1

照射線量	C/kg	R
	1	3876
	2.58 × 10^{-4}	1

線量当量	Sv	rem
	1	100
	0.01	1

(86年12月26日現在)

Performance Test of Micro-fission Chambers for In-vessel Neutron Monitoring of ITER